



STUDIECENTRUM VOOR KERNENERGIE
CENTRE D'ÉTUDE DE L'ÉNERGIE NUCLÉAIRE



(Unclassified)

Mechanical Characterization of EUROFER97 Irradiated to 0.32 dpa at 300 °C

EFDA Technology Workprogramme 2001
Tritium Breeding and Materials
Materials Development - TTMS-001

E. Lucon, A. Leenaers

RMO
SCK·CEN, Mol, Belgium

BLG-896

March 2002

DISTRIBUTION LIST

A. Al-Mazouzi	SCK•CEN – RMO	1
R. Chaouadi	SCK•CEN – RMO	1
A. Leenaers	SCK•CEN – RMO	1
E. Lucon	SCK•CEN – RMO	1
L. Malerba	SCK•CEN – RMO	1
J.-L. Puzzolante	SCK•CEN – RMO	1
J. Schuurmans	SCK•CEN – RMO	1
M. Scibetta	SCK•CEN – RMO	1
S. Van Dyck	SCK•CEN – RMO	1
E. van Walle	SCK•CEN – RMO	1
M. Décreton	SCK•CEN – BR3	1
M. Gasparotto	EFDA, Garching (D)	2
G. Lemarois	EFDA, Garching (D)	1
B. Van Der Schaaf	NRG, Petten (NL)	1
	Secretariaat RMO	3

This document has been written and approved by:

		Date	Approval
Authors:	E. Lucon	14/3/02	<i>E. Lucon</i>
	A. Leenaers	14/3/02	<i>A. Leenaers</i>
Verified by:	M. Scibetta	14/3/02	<i>M. Scibetta</i>
	A. Almazouzi	14/03/02	<i>A. Almazouzi</i>
Fusion Coordinator:	M. Décreton	15/03/02	<i>M. Décreton</i>
Approved by:	E. van Walle	14/03/02	<i>E. van Walle</i>

RESTRICTED

All property right and copyright are reserved. Any communication or reproduction of this document, and any communication or use of its content without explicit authorization is prohibited. Any infringement to this rule is illegal and entitles to claim damages from the infringer, without prejudice to any other right in case of granting a patent of registration in the field of intellectual property. SCK•CEN, Boeretang 200, B-2400 Mol.

(Unclassified)

Mechanical Characterization of EUROFER97 Irradiated to 0.32 dpa at 300 °C

EFDA Technology Workprogramme 2001
Tritium Breeding and Materials
Materials Development - TTMS-001

E. Lucon, A. Leenaers

BLG-896

RMO
SCK•CEN, Mol, Belgium

March 2002

TABLE OF CONTENTS

1	Introduction	3
2	Material and irradiation conditions.....	3
3	Tensile test results.....	4
	<i>3.1 Comparison with unirradiated tensile data.....</i>	<i>6</i>
4	Impact test results.....	9
	<i>4.1 Comparison with unirradiated impact test data.....</i>	<i>14</i>
5	Fracture toughness test results	15
	<i>5.1 Comparison with unirradiated fracture toughness data</i>	<i>17</i>
6	Summary of irradiation effects and comparison with other RAFM steels.....	21
	<i>6.1 Tensile properties.....</i>	<i>21</i>
	<i>6.2 Impact properties</i>	<i>23</i>
	<i>6.3 Fracture toughness properties.....</i>	<i>24</i>
	CONCLUSIONS	25
	ACKNOWLEDGEMENTS	25
	REFERENCES	26
	Appendix 1.....	31
	Appendix 2.....	356
	ANNEX 1	

ABSTRACT

The reduced-activation ferritic martensitic steel EUROFER97 (9CrWVTa) is the main structural material presently considered for the Breeding Blankets Modules of DEMO and will be used for the Test Blankets Modules developed in the EU. Its specification results from a 20 year R&D effort and collaborative work performed under the auspices of the International Energy Agency.

Mechanical specimens extracted from a forged bar (heat n° E83699) have been irradiated in the BR2 reactor at 300 °C up to a fluence of 2.14×10^{20} n/cm² (E > 1 MeV), in the frame of the IRFUMA-I experiment. Tensile, impact and fracture toughness test results have been obtained from the irradiated samples, allowing to assess the consequences of neutron exposure on the mechanical strength (hardening) and toughness properties (embrittlement) of the material, after comparison with data available for the unirradiated condition.

In spite of the limited amount of relevant data available in the open literature, the effects of irradiation on EUROFER97 have been compared with those observed on other RAFM steels (F82H in particular), under comparable irradiation conditions.

KEYWORDS

Reduced-activation ferritic martensitic (RAFM) steels, EUROFER97, irradiation, IRFUMA-I, hardening, embrittlement, F82H.

1 Introduction

The development of structural materials for fission reactors has followed an evolutionary path, constantly building upon the experience acquired from previous generations.

The development of structural materials for the fusion power reactors can also benefit from the fission experiences, but in some cases (such as vessel and in-vessel components) has to rely on its own evolutionary path. This will be achieved through the construction of ITER, the testing of Blanket Modules in ITER and the development of a demonstration reactor (DEMO).

However, since the transition from ITER or DEMO to a commercial power reactor would involve significant changes in system and material options, the European R&D program includes also a parallel path investigating more advanced materials, as well as provisions for an intense neutron source facility (IFMIF) for testing all candidate materials.

A wide range of materials is presently investigated for ITER and DEMO [1-4], including conventional materials (austenitic stainless steels, Cu alloys, Ti alloys, Cr alloys), low-activation structural materials (ferritic-martensitic steels including ODS, Va alloys, ceramic composites) and materials for high heat flux regions (W and CFC).

Among high temperature materials for first wall and blanket components, Reduced-Activation Ferritic Martensitic (RAFM) steels have presently a prominent role in European and worldwide R&D activities [3,5]. Several conventional grades are already qualified, such as T91; one of the RAFM steels currently investigated, F82H (Fe-8Cr-2W-Ta-V), has already a good data base [6,7].

In an effort to improve the toughness while retaining the mechanical strength of F82H, EUROFER97 (Fe-9Cr-1W-Ta-V) has been developed as the RAFM steel preferred and extensively studied in Europe, presently in its early stage of characterization [5]. This report presents the results of the mechanical characterization of this steel, after irradiation in the BR2 reactor in Mol to 2.14×10^{20} n/cm² (0.32 dpa) at 300 °C, and compares irradiated test results to unirradiated data previously obtained by other European institutions in the frame of the EFDA Tritium Breeding and Materials Materials Development Programme.

The irradiation conditions of the IRFUMA-I experiment (temperature and dose) are not representative of the foreseen service conditions of ITER or DEMO structural materials (much higher doses and temperatures); however, investigations such as the present one are considered to be important steps in the characterization of the material's irradiation sensitivity.

2 Material and irradiation conditions

The EUROFER97 steel has been modelled after the conventional T91 alloy, by selectively replacing some elements which would transmute in a fusion neutron spectrum into high-energy radiation emitters with long half-life; for instance, W replaced Mo and Ta substituted for Nb. Such replacements have no significant impact on mechanical properties but result beneficial from a radiological point of view.

Its tempered martensitic microstructure allows operation at relatively high temperatures (up to 500 – 550 °C) and offers a good dimensional stability under high neutron dose level conditions. Moreover, it exhibits higher swelling resistance than austenitic steels, about 1% volume per 100 dpa as compared to about 1% volume per 10 dpa [8].

The strength of RAFM steels at high temperature can be improved through the use of Oxide Dispersion Strengthened (ODS) grades, containing a fine dispersion of small oxide particles (Y_2O_3 and/or TiO_2) in a ferrite matrix. These are currently being developed and characterized in Japan, United States and Europe; most of the work in Japan [9] and US [10] is concentrated on higher Cr content steels, whereas in Europe EUROFER97 ODS steels are being produced [12] and preliminarily characterized [13,14].

EUROFER97 has been produced by Böhler AG in various product forms (plates and bars), in order to demonstrate the feasibility of the industrial production route. Plates were fabricated with thicknesses of 8, 14 and 25 mm; the six forged bars had a diameter of 100 mm.

SCK•CEN received from FZK Karlsruhe a portion of one of the forged bars (heat n°E83699). The inspection certificate issued by Böhler AG, which contains information about chemical composition, heat treatment, mechanical properties and other characteristics of the bar has been given in Appendix 1. The remaining portions of the bars were distributed amongst other institutions (CEA Grenoble, CEA Saclay, NRG) or retained by FZK Karlsruhe.

Tensile, Charpy-V impact and precracked Charpy-V specimens have been extracted from the bar in the longitudinal direction; the cutting scheme is given in Appendix 2 (block 2).

The specimens were loaded into the Callisto rig of the BR2 reactor of Mol, in the frame of the irradiation campaign denominated IRFUMA-I; irradiation was performed in the last cycle of 2000 (November/December), at a nominal temperature of 300 ± 5 °C. Irradiation conditions have been described in detail in a separate report [15].

Detailed dosimetry measurements have been carried out and reported elsewhere [16]; the measured average fast neutron fluence is 2.14×10^{20} n/cm² ($E > 1$ MeV), corresponding to **0.32 dpa**.

An overview of the mechanical tests performed is given in Table 1.

Table 1 - *Tests performed on the EUROFER97 specimens irradiated in IRFUMA-I.*

Type of test	No of tests performed	Average fluence (n/cm ² , E>1 MeV)	Average dose (dpa)	Temperature range (°C)
Tensile	12	2.31×10^{20}	0.35	-150 ÷ 300
Impact	12	2.06×10^{20}	0.31	-80 ÷ 25
Toughness	18	2.08×10^{20}	0.31	-110 ÷ -50

3 Tensile test results

Twelve tensile specimens of cylindrical cross section (diameter $D = 3$ mm, reduced section length $L_0 = 15$ mm) have been tested from -150 °C to 300 °C, according to the requirements of ASTM E8M standard. No extensometer has been used for measuring specimen elongation.

Test results are given in Table 2, in terms of yield strength ($\sigma_{p0.2}$), ultimate tensile strength (σ_{UTS}), uniform elongation (ϵ_u), total elongation (ϵ_t) and reduction of area (Z).

Tensile strengths have been fitted as a function of test temperature, obtaining the following expressions:

$$\sigma_{p0.2} = 578.6 + 87.4 \cdot e^{-0.01028T}$$

for the yield strength, and

$$\sigma_{UTS} = 583.9 + 151.1 \cdot e^{-0.00661T}$$

for the ultimate tensile strength. This fitting functions are relevant only to the test temperature range, and should not be extrapolated to higher temperatures (i.e. above 300 °C).

Table 2 - Results of the tensile tests on irradiated EUROFER97.

T [°C]	σ_{p02} [MPa]	σ_{UTS} [MPa]	ϵ_u [%]	ϵ_t [%]	Z [%]
-150	1001	1001	N/A	24	74
-150	984	993	7	23	70
-75	745	818	8	22	75
-75	753	816	7	21	76
30	672	720	5	18	80
32	650	708	6	18	79
150	619	654	4	16	81
150	610	656	5	17	80
225	579	610	2	14	81
225	585	620	3	14	81
300	569	593	1	13	81
300	562	597	2	13	82

Figure 1 and Figure 2 show the trend of tensile strengths and ductility parameters, respectively, with temperature.

It can be observed that EUROFER97 retains elevated mechanical strength and good ductility after irradiation to 0.32 dpa.

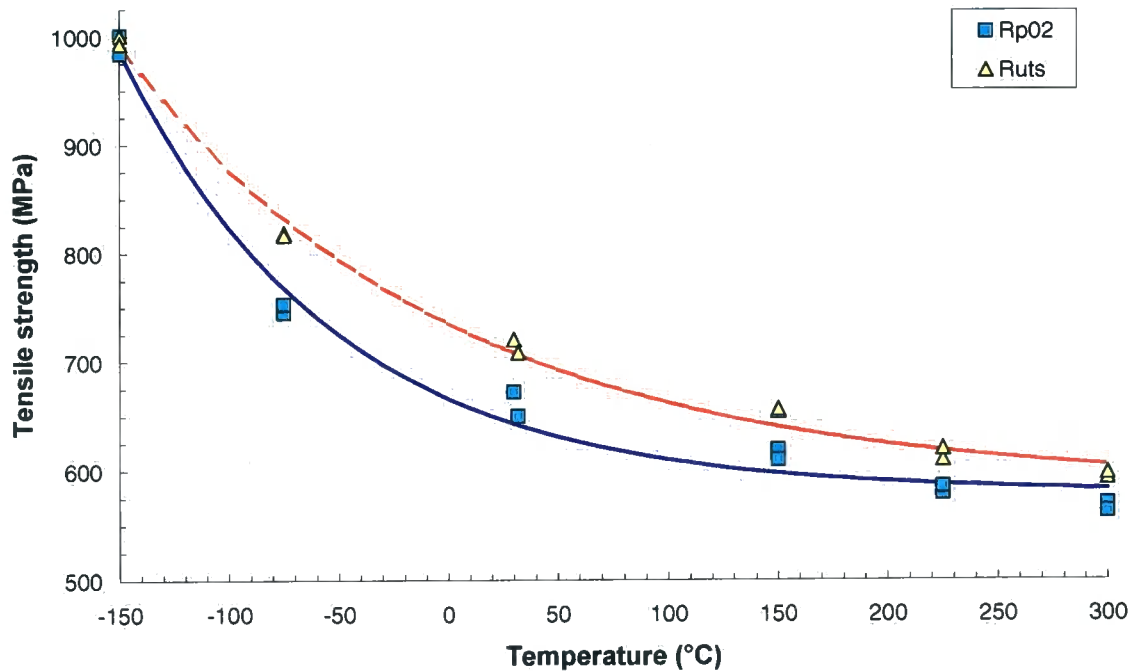


Figure 1 - Values of tensile strengths measured as a function of temperature for the irradiated EUROFER97.

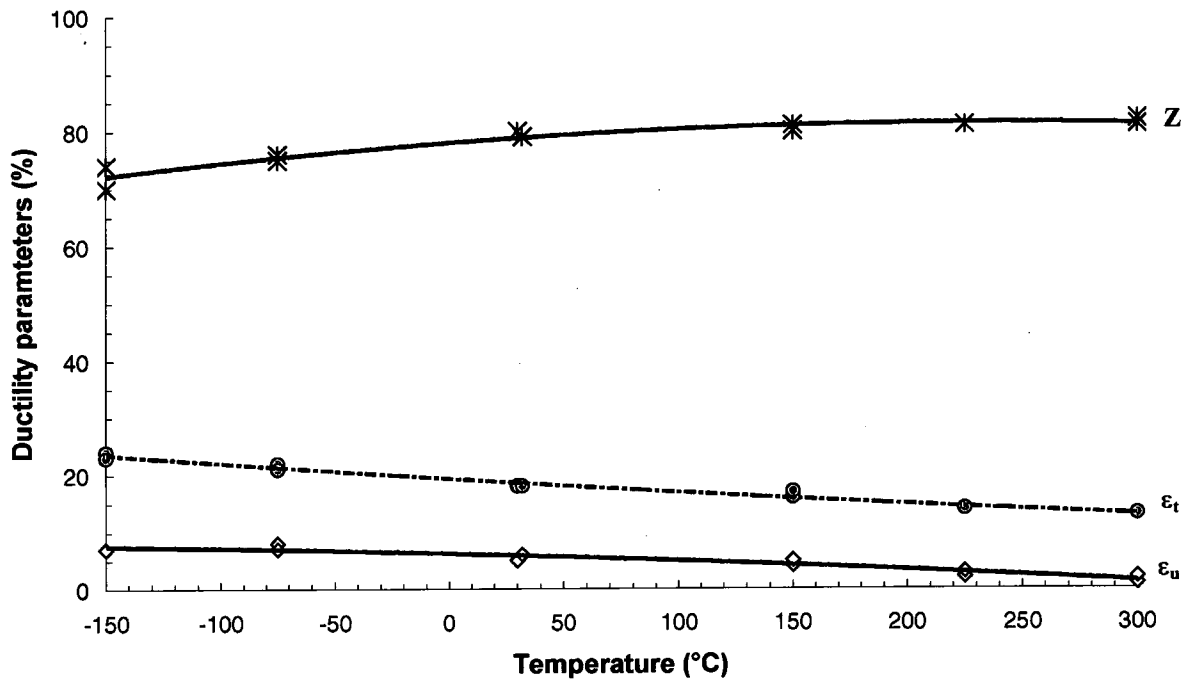


Figure 2 - Values of ductility parameters measured as a function of temperature for the irradiated EUROFER97.

3.1 Comparison with unirradiated tensile data

Tensile test results from the EUROFER97 forged bars in the baseline (unirradiated) condition are presently available from NRG (Petten, NL) [17] and FZK (Karlsruhe, D) [18,19]; additionally, baseline tensile data from the plates with 14 mm thickness, which were found to have mechanical properties very similar to those of the bars, have been reported from NRG, FZK and CEA (Saclay, France) [20].

The comparison between unirradiated and irradiated data, in terms of yield strength, ultimate tensile strength, uniform elongation, total elongation and reduction of area is given in Figure 3 to Figure 7, respectively. An assessment of the change in measured values as a consequence of neutron exposure is only possible in the temperature range R.T. ÷ 300 °C, where the test intervals overlap.

The irradiation-induced hardening of EUROFER97 is approximately 100 MPa or 20% in terms of yield strength increase (Figure 3), while the augmentation of the ultimate tensile strength is smaller (from 35 to 55 MPa or from 5% to 10%, Figure 4). No visible decrease of uniform elongation and reduction is observed (Figure 5 and Figure 7, respectively), while total elongation is moderately affected (reduction between 3% and 4.5%, Figure 6).

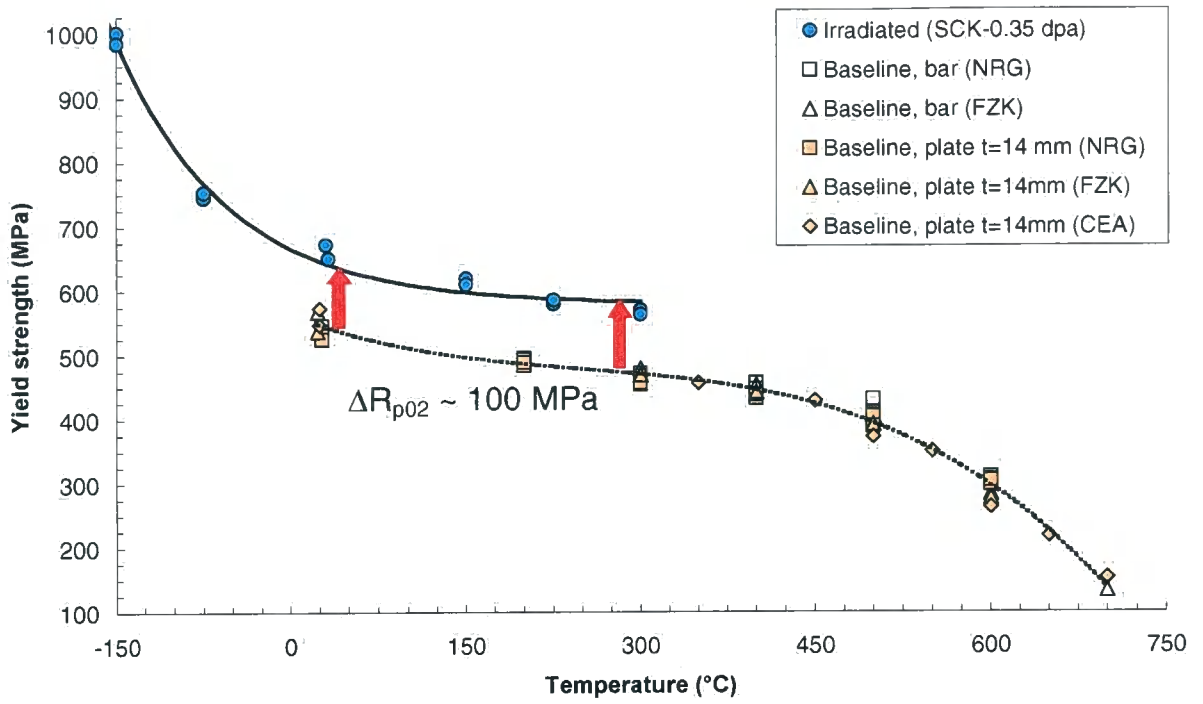


Figure 3 - Comparison between baseline and irradiated EUROFER97 in terms of yield strength.

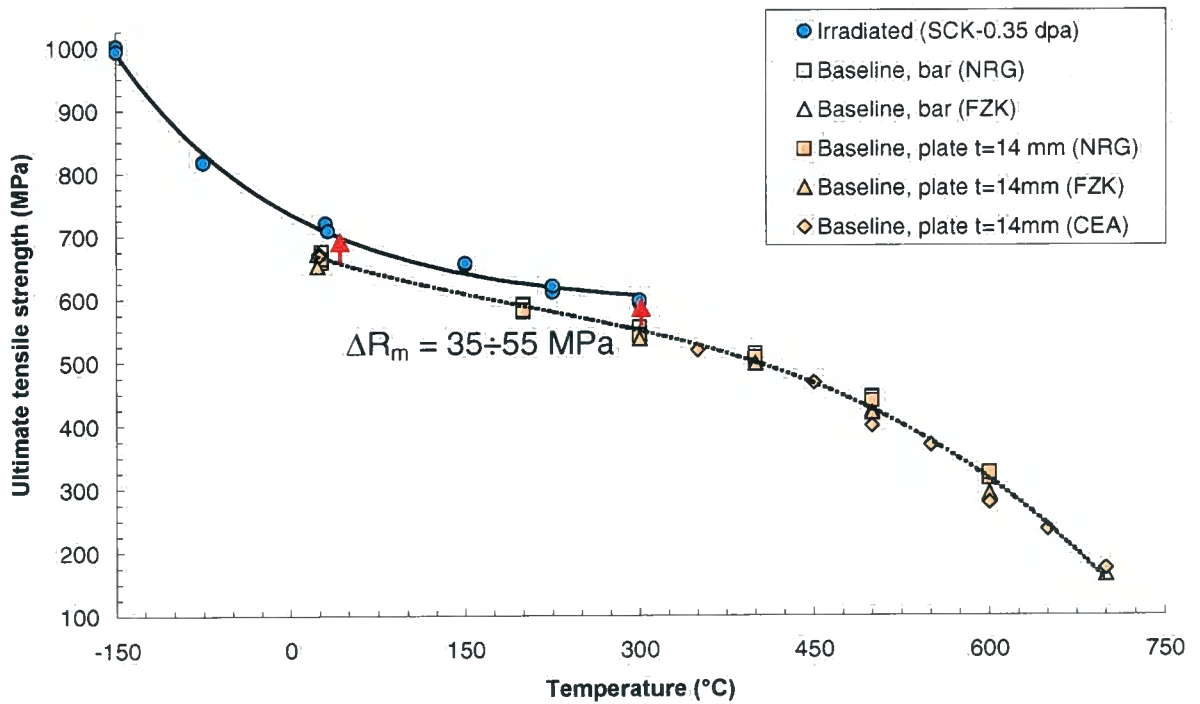


Figure 4 - Comparison between baseline and irradiated EUROFER97 in terms of ultimate tensile strength.

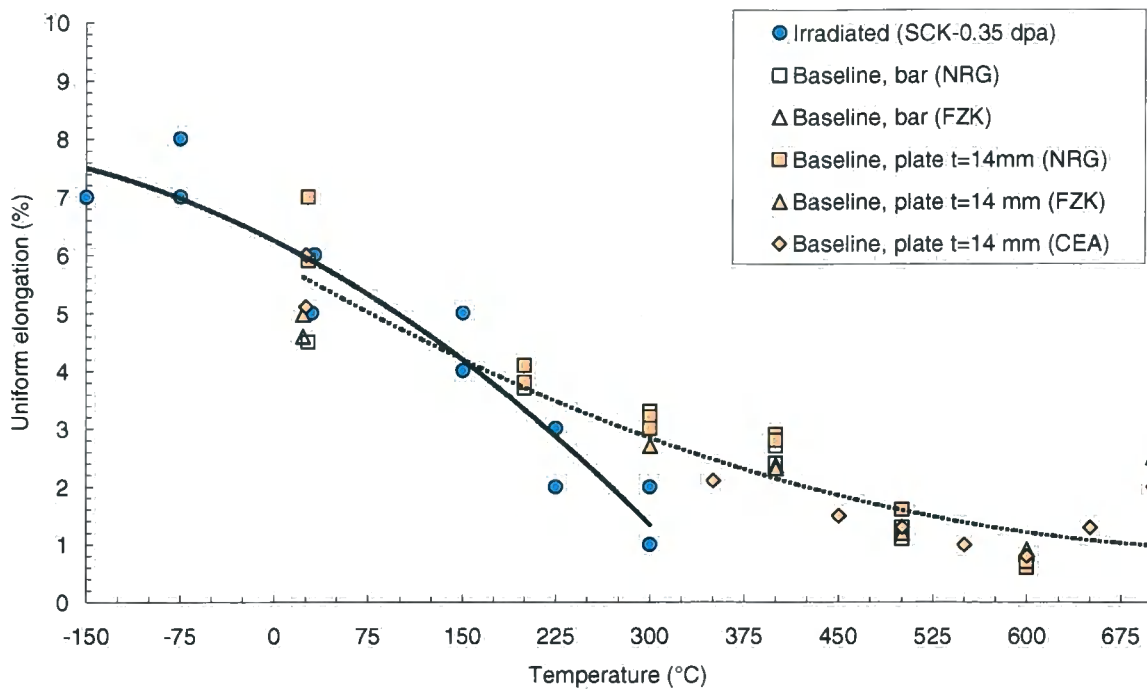


Figure 5 - Comparison between baseline and irradiated EUROFER97 in terms of uniform elongation.

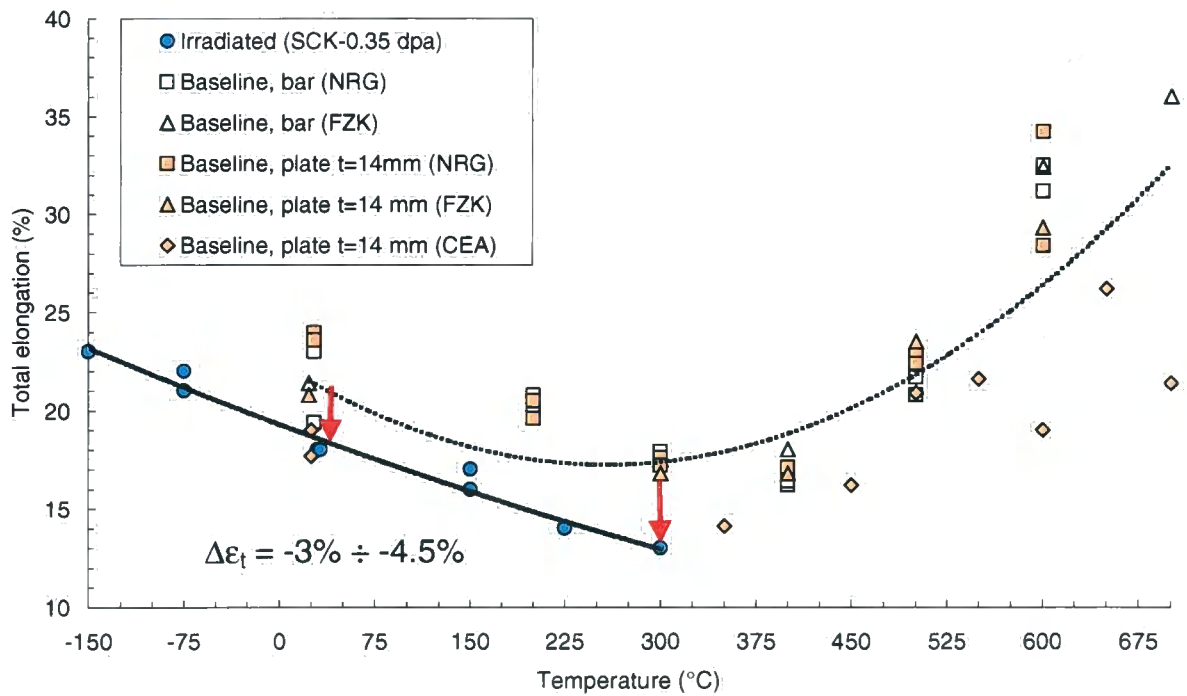


Figure 6 - Comparison between baseline and irradiated EUROFER97 in terms of total elongation.

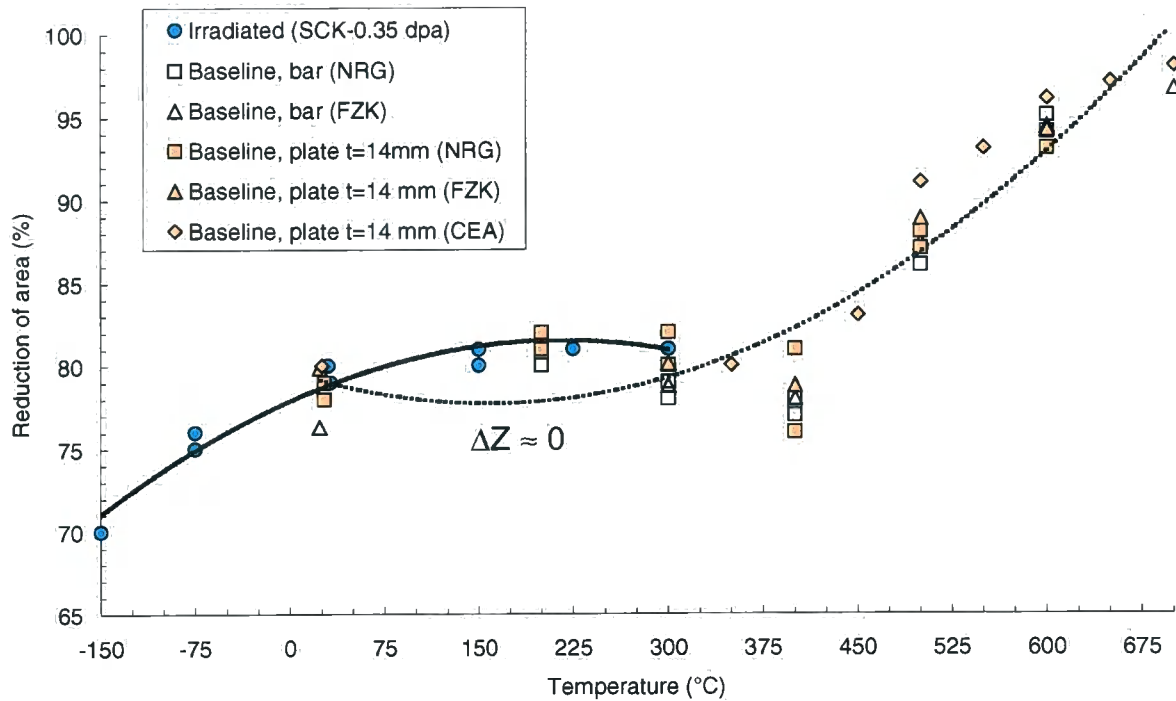


Figure 7 - Comparison between baseline and irradiated EUROFER97 in terms of reduction of area.

4 Impact test results

Twelve Charpy impact specimens (V-notch, standard type) have been tested from -80 °C to 25 °C, in order to derive full transition curves for absorbed energy, shear fracture appearance (SFA) and lateral expansion (LE). Tests were performed on a 300 J Wolpert pendulum, equipped with an instrumented striker complying with the requirements of the ISO 14556 standard.

Test results are given in Table 3.

Table 3 - Results of impact tests performed on irradiated EUROFER97.

Specimen Code	T (°C)	Energy (J)	SFA (%)	LE (mm)
E97-07	-80	5.7	0	0.109
E97-03	-50	13.5	5	0.236
E97-10	-50	23.7	6	0.391
E97-12	-47.5	181.1	64	2.452
E97-09	-45	171.1	62	2.072
E97-06	-40	188.1	63	2.379
E97-08	-40	200.8	74	2.337
E97-05	-30	209.8	80	2.409
E97-04	-20	206.7	83	2.402
E97-11	-20	223.3	77	2.235
E97-02	0	286.7	100	2.409
E97-01	25	268.0	100	2.467

Test results have been fitted with the well-known hyperbolic tangent (TANH) model, in order to derive characteristic parameters such as the Ductile-to-Brittle Transition Temperature (DBTT) and the Upper Shelf Energy (USE). This function has the following analytical expression:

$$P(T) = A + B \tanh\left(\frac{T - DBTT}{C}\right)$$

where: $P(T)$ is the fitted function; A , B , C are fitting coefficients; $(A + B)$ corresponds to the Upper Shelf value, which is given by the average of specimen exhibiting $SFA \geq 95\%$; $(A - B)$ corresponds to the Lower Shelf value, and has been fixed to 2.7 J and 0.061 mm for energy and lateral expansion, respectively [21].

However, the TANH function doesn't seem to do a good job in fitting absorbed energy data, which exhibit an abrupt transition from the lower shelf and a more gradual transition to the upper shelf (Figure 8).

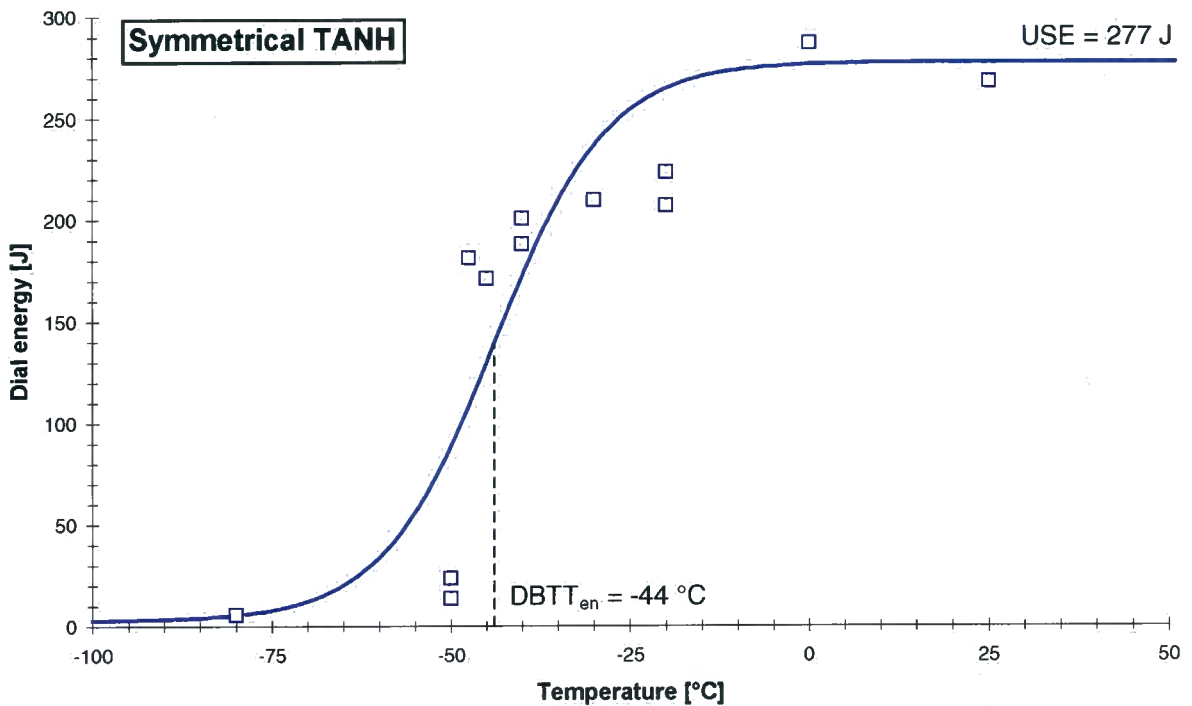


Figure 8 - Energy data obtained on irradiated EUROFER97 (fitted with TANH function).

Two alternative analytical functions have therefore been used for fitting energy data:

- asymmetric hyperbolic tangent function (ATANH, Figure 9) [22]:

$$P(T) = A + B \tanh\left(\frac{T - DBTT}{D \cdot T + C}\right)$$

where D is an additional fitting coefficient;

- modified exponential function (PHI, Figure 10) [23]:

$$P(T) = A + \frac{B}{1 + e^{\frac{DBTT - T}{C}}} \cdot \frac{1}{(T + 273.15)^n}$$

where: A, B, C and n are fitting coefficients; A corresponds to the Lower Shelf value, while the Upper Shelf level is not defined, since the PHI function has an increasing (for $n < 0$) or decreasing (for $n > 0$) trend in the Upper Shelf region.

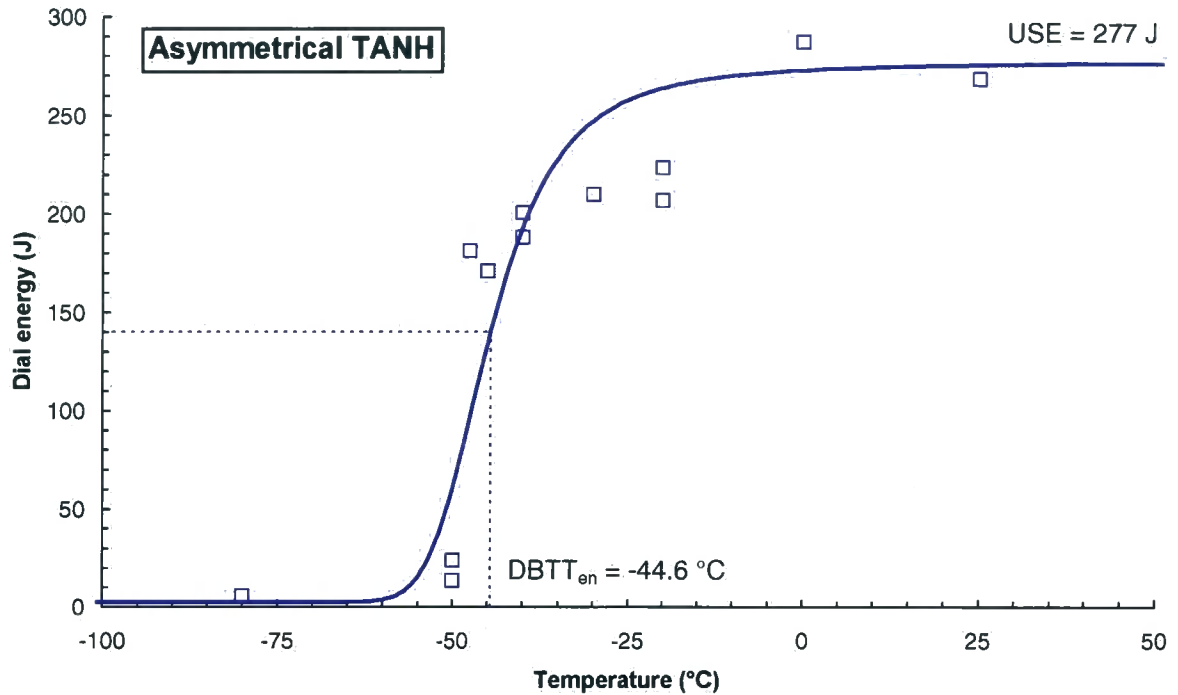


Figure 9 - Energy data obtained on irradiated EUROFER97 (fitted with ATANH function).

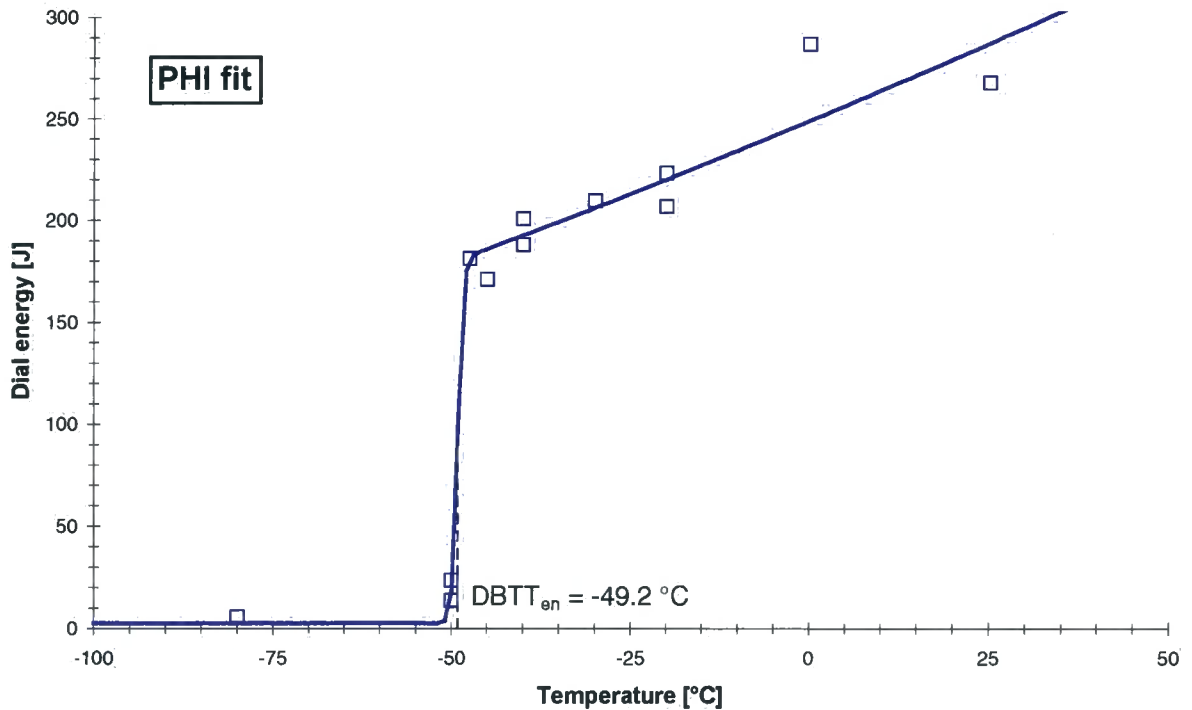


Figure 10 - Energy data obtained on irradiated EUROFER97 (fitted with PHI function).

Shear Fracture Appearance and Lateral Expansion data, on the other hand, have been fitted using the conventional TANH approach (Figure 11 and Figure 12).

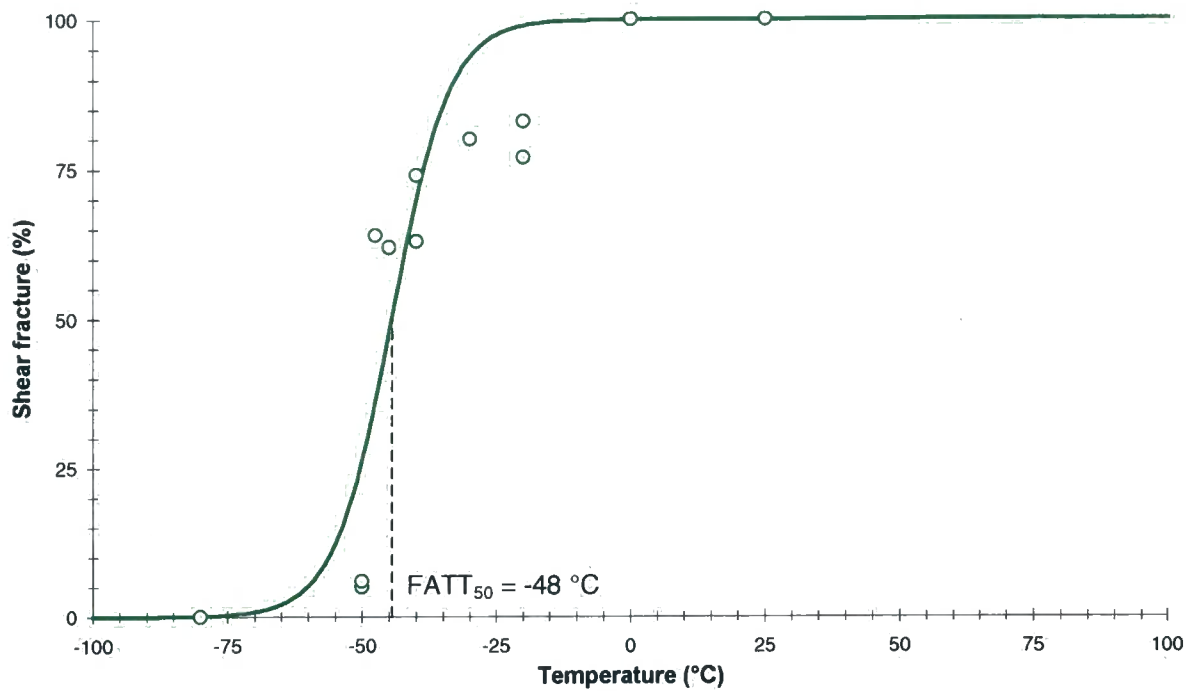


Figure 11 - SFA data obtained on irradiated EUROFER97 (fitted with TANH function).

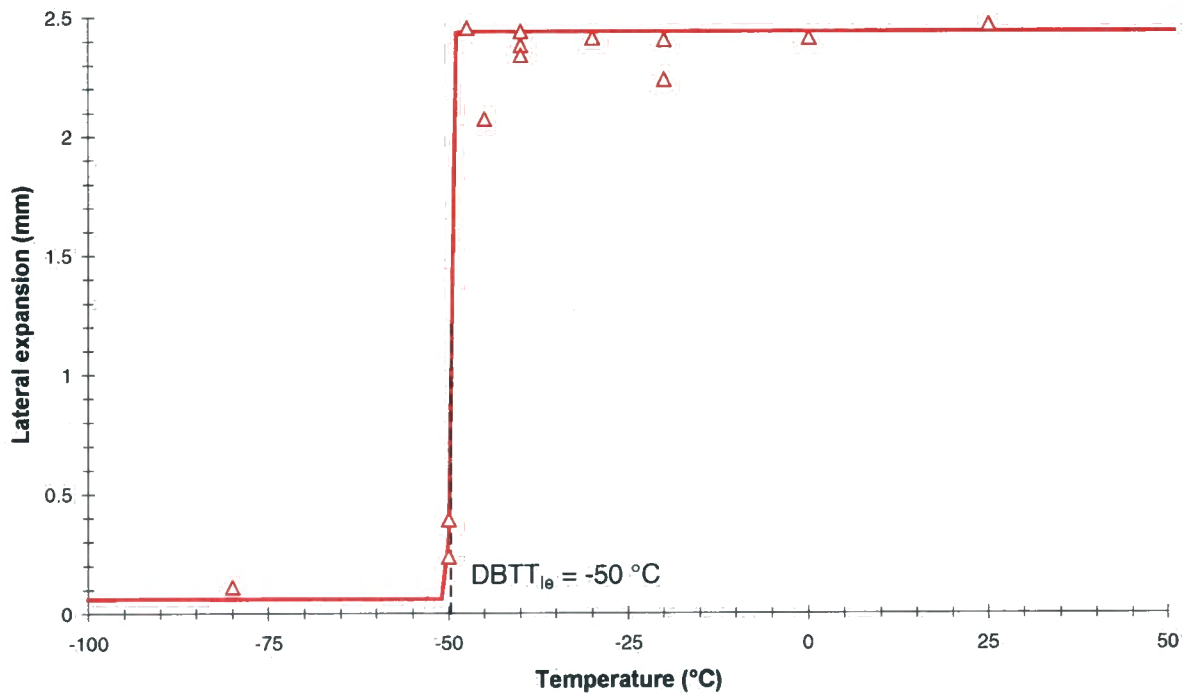


Figure 12 – Lateral expansion data obtained on irradiated EUROFER97 (fitted with TANH function).

Table 4 summarizes the values of transition temperatures and Upper Shelf Energy obtained by fitting the experimental data.

Table 4 - Transition temperatures and USE calculated on irradiated EUROFER97.

Parameter	Model	DBTT (°C)	USE (J)	Sum of Square Residuals
Absorbed energy	TANH	-44.0	277.4	1990.94
	ATANH	-44.6	277.4	1569.37
	PHI	-49.2	-	196.37
Shear Fracture Appearance	TANH	-44.5	-	236.07
Lateral Expansion	TANH	-49.8	-	0.017

As far as fitting energy data is concerned, the use of the ATANH model gives only a moderate improvement over the TANH function; however, the PHI model reduces the Sum of Square Residuals by an order of magnitude. Therefore, the DBTT value provided by this function (-49.2 °C) is assumed for use in further analyses.

Another significant issue is represented by the USE value, which is determined by the two specimens tested at the highest temperatures (0 and 25 °C).

For both these specimens, the absorbed energy is higher than 240 J (80% of the range of the pendulum used).

To this regard, the ASTM E23 standard states that "the upper limit of the usable range of the machine is equal to 80% of the capacity of the machine" (§ A2.4.3.2).

Furthermore, recent studies [24] have shown that excess machine capacity (i.e. the difference between the pendulum full range and the energy absorbed by the specimens) has a critical effect on the impact toughness. Specifically, high-energy steels tested in the upper 20% of the machine range show an "apparent toughness" significantly higher than when tested on a higher capacity machine (Figure 13).

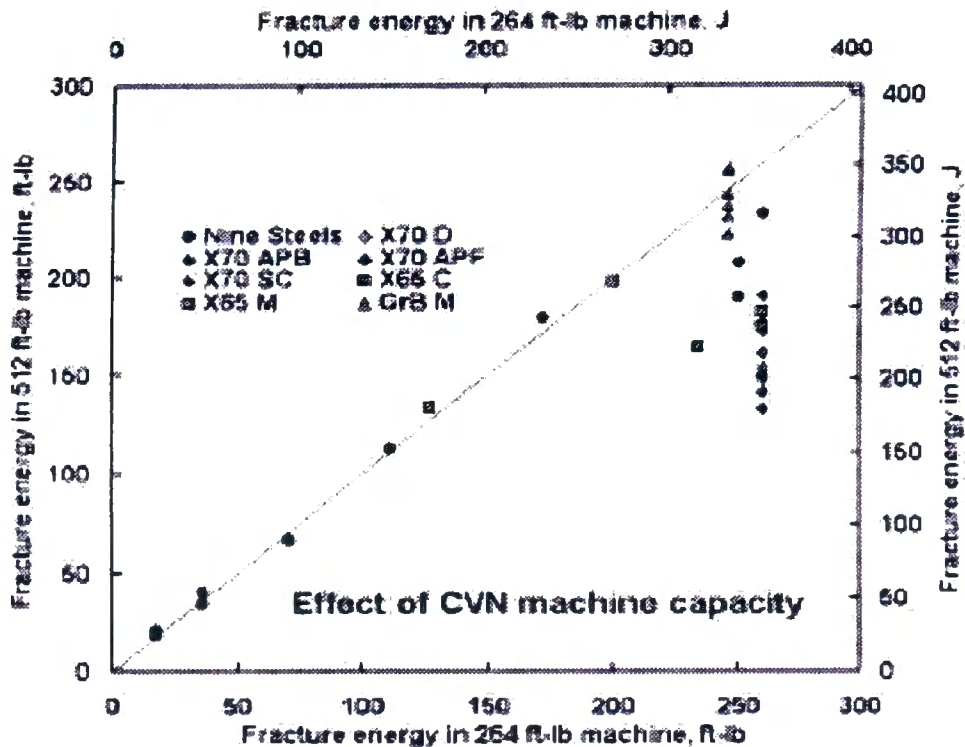


Figure 13 - Effect of machine excess capacity on absorbed energy [24].

Consequently, the absolute Upper Shelf Energy value measured on the irradiated EUROFER97 and reported in Table 4 is probably overestimated and should be considered not reliable. Further impact tests in the same temperature range should be carried out on a larger capacity machine.

However, from an engineering viewpoint, the USE level remains high, therefore implying that under these conditions failure by ductile tearing does not represent a critical issue.

4.1 Comparison with unirradiated impact test data

Baseline impact test results, obtained from full-size Charpy specimens extracted from the forged bars, are presently only available from FZK [18,19].

More full-size Charpy data from the 14 mm thick plate have been reported by CEA [20] and CIEMAT [25], as well as by FZK. As previously mentioned, FZK test results demonstrate the equivalence of bar and plate $t = 14$ mm in terms of mechanical properties.

Moreover, NRG has also characterised both product forms, but using KLST sub-size Charpy specimens [17]; however, reliable correlations between full-size and sub-size Charpy specimens have yet to be established for this class of steels.

Baseline and irradiated impact data are compared in Figure 14 (energy) and Figure 15 (SFA), along with respective fitting curves.

The DBTT shift caused by neutron irradiation is $14\text{ }^{\circ}\text{C}$ in terms of energy and $16\text{ }^{\circ}\text{C}$ in terms of SFA.

As far as USE values are concerned, Figure 14 shows an apparent augmentation of Upper Shelf Energy with irradiation, contrary to what is normally observed. However, as previously explained, the absolute value of irradiated USE is not reliable and should not be used for assessing the effects of neutron exposure. It seems however reasonable to assume a limited effect of irradiation on the Upper Shelf Energy level.

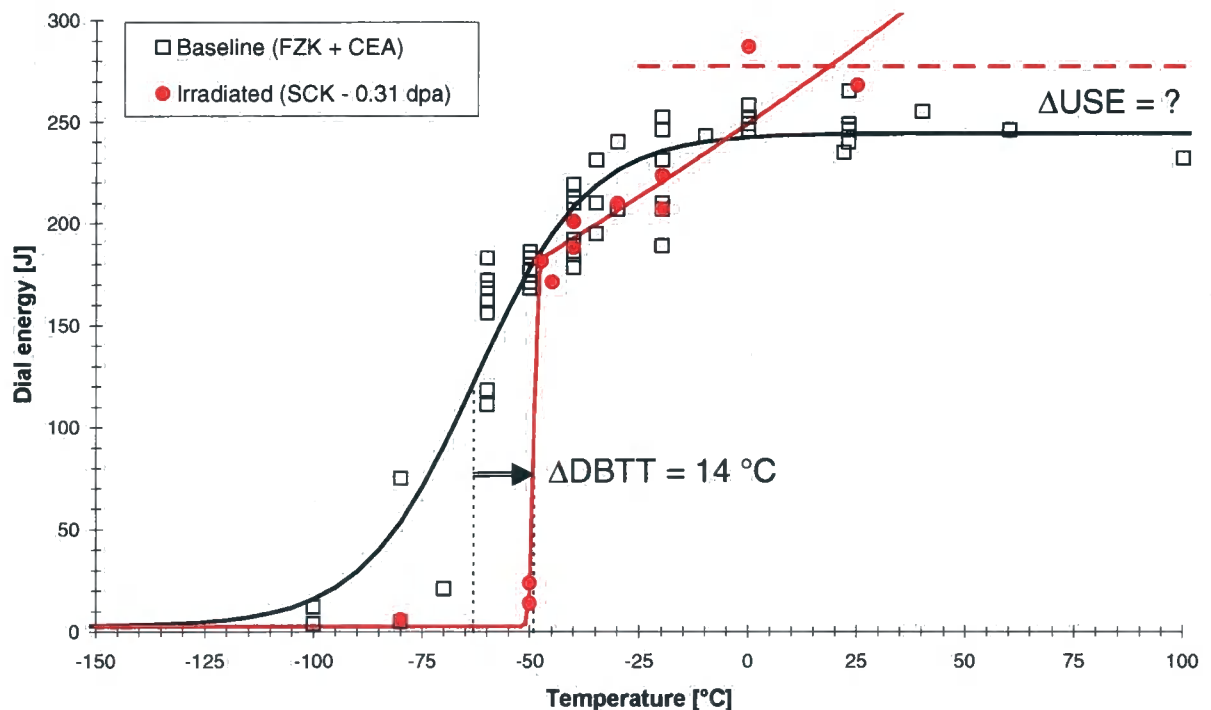


Figure 14 - Comparison between absorbed energy data from baseline and irradiated EUROFER97.

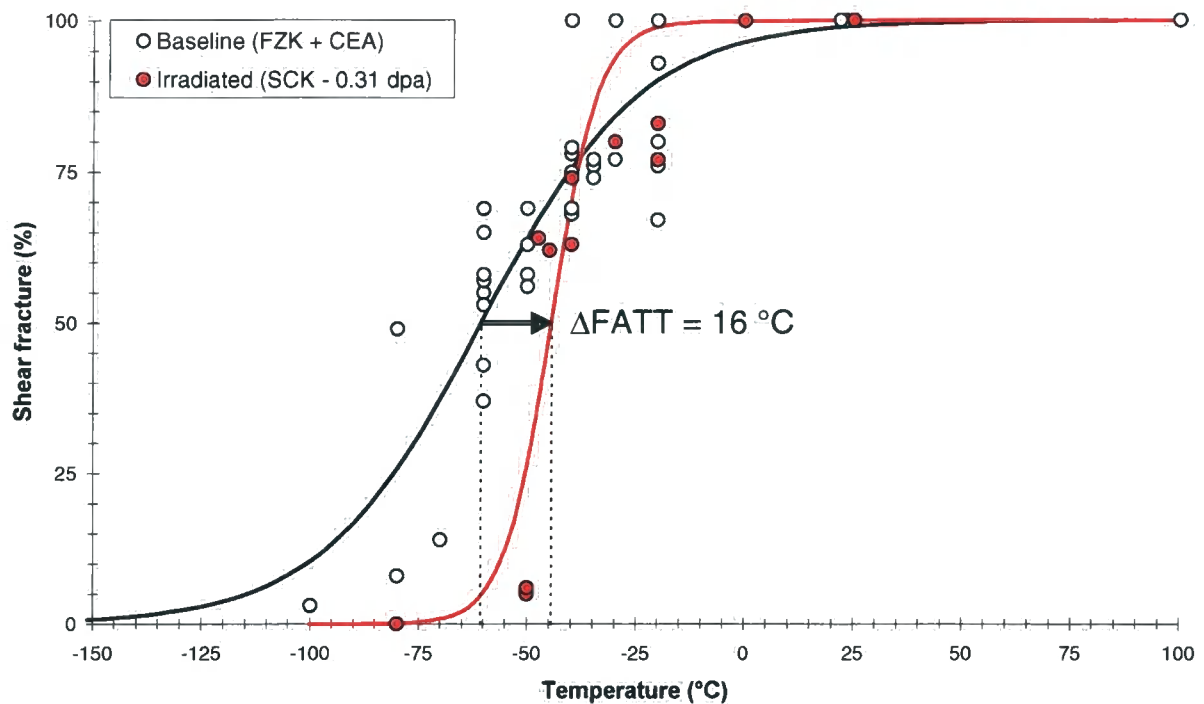


Figure 15 - Comparison between Shear Fracture Appearance data from baseline and irradiated EUROFER97.

5 Fracture toughness test results

Eighteen fatigue precracked Charpy specimens (V-notch, standard type) have been tested from -110 °C to -50 °C , in order to derive a valid reference temperature corresponding to a toughness level of $100\text{ MPa}\sqrt{\text{m}}$ for a 1TCT specimen, in accordance with the ASTM E1921-01 standard (multi-temperature option). It should be emphasized that, strictly speaking, the E1921 is applicable to ferritic steels only; however, evidence exists that the methodology is amenable to ferritic-martensitic steels as well, which have a BCC crystalline structure and exhibit a clear ductile-to-brittle transitional behaviour.

Nine of the tests have been performed at -70 °C , obtaining another value of reference temperature (single-temperature option).

Individual test results are given in Table 5, while Table 6 shows the results of the analyses according to the Master Curve methodology. Figure 16 shows normalised experimental data points with the relevant Master Curve and associated confidence bounds.

All specimens were plain-sided (without side-grooves), and were tested in displacement control at a speed of 0.2 mm/min using an electromechanical testbank.

Both calculated reference temperatures (multi-T and single-T) are valid according to the ASTM E1921-01 standard.

Table 5 - Individual results for fracture toughness tests on irradiated EUROFER97.

Specimen code	T (°C)	W (mm)	B (mm)	a ₀ (mm)	Δa (mm)	K _{Jc} (MPa√m)	DATA VALID
E97-16	-110	10.011	10.012	5.022	0.00	60.0	YES
E97-17	-90	10.011	10.011	5.536	0.00	60.0	YES
E97-30	-80	10.011	10.012	4.587	0.00	168.7	YES
E97-31	-80	10.015	10.015	4.759	0.00	89.9	YES
E97-32	-80	10.009	10.009	4.823	0.00	108.1	YES
E97-33	-80	10.018	10.018	4.828	0.00	104.8	YES
E97-18	-70	10.006	10.009	4.853	0.00	110.7	YES
E97-19	-70	10.016	10.014	4.801	0.00	112.4	YES
E97-23	-70	10.010	10.010	4.110	0.24	240.5	NO (K _{Jc} > K _{lim})
E97-24	-70	10.014	10.012	5.131	0.00	109.9	YES
E97-25	-70	10.008	10.010	4.719	0.21	224.5	NO (K _{Jc} > K _{lim})
E97-26	-70	10.018	10.014	4.859	0.00	153.3	YES
E97-27	-70	10.005	10.006	4.879	0.00	94.3	YES
E97-28	-70	10.020	10.018	4.476	0.28	297.4	NO (K _{Jc} > K _{lim})
E97-29	-70	10.011	10.011	4.119	0.00	108.0	YES
E97-20	-50	10.014	10.014	4.950	0.00	103.0	YES
E97-21	-50	10.014	10.017	4.931	0.00	229.7	NO (K _{Jc} > K _{lim})
E97-22	-50	10.014	10.014	4.644	0.58	355.2	NO (K _{Jc} > K _{lim})

W, B = specimen width and thickness; a₀ = initial crack length; Δa = ductile crack extension; K_{Jc} = fracture toughness measured at cleavage; K_{lim} = fracture toughness validity limit according to ASTM E1921-01.

Table 6 - Results of the Master Curve analyses for the irradiated EUROFER97.

Option	N	r	K _{o,1TCT} (MPa√m)	K _{med,1TCT} (MPa√m)	T _o (°C)
Multi-T	18	13	122.2	113.2	-80
Single-T	9	6	131.6	121.8	-84

N = number of specimens tested, r = number of valid data; K_{o,1TCT} = scale parameter of the distribution (normalised); K_{med,1TCT} = median value of the population (normalised); T_o = reference temperature.

Considering the average of the multi-temperature and single-temperature options, the reference temperature for the EUROFER97 steel in the irradiated condition (0.31 dpa) is the following:

$$T_o = -82^\circ\text{C}$$

with an associated standard deviation of 5 °C.

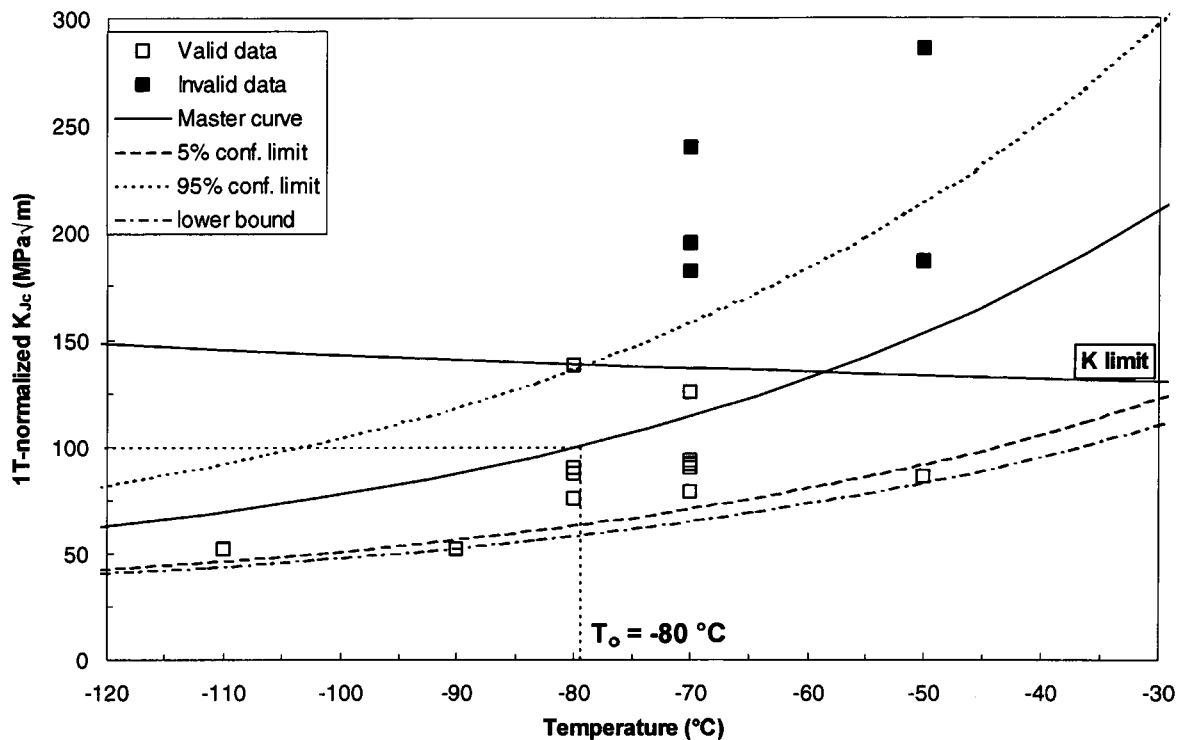


Figure 16 - Normalised fracture toughness data with Master Curve and associated confidence bounds (multi-T option) for the irradiated EUROFER97.

5.1 Comparison with unirradiated fracture toughness data

Only two institutes have so far reported fracture toughness data obtained in the baseline condition:

- NRG Petten tested C(T) specimens with thicknesses $B = 5$ mm and 10 mm, extracted from the 25 mm thick plate [26];
- CIEMAT reported fracture toughness results obtained from 1/2TCT specimens from the plate with $t = 14$ mm [25].

In both cases, tests were performed in the ductile-to-brittle transition regime and data were analyzed according to the Master Curve methodology in order to obtain the reference temperature T_0 . However, both datasets are not directly comparable to the results obtained by SCK•CEN, since:

- both institutes have used Compact Tension specimens, which are known to possess slightly higher crack-tip constraint than Precracked Charpy-V samples (and bend-type specimens in general) [27,28]: in terms of Master Curve analysis, this usually results in a 10 °C difference in reference temperature ($T_{0,C(T)} - T_{0,PCCV} \approx 10$ °C) [29,30];
- the mechanical properties of the 25 mm EUROFER97 plate have been found to be inferior to all other product forms (bars, plates $t = 8$ mm and $t = 14$ mm) [17]: based on Charpy results, the DBTT shift is around 22 °C.

Therefore, although correlations with NRG and CIEMAT data can be used, in order to assess directly the reference temperature shift induced by neutron irradiation some fracture toughness tests in the baseline condition have been carried out using precracked Charpy specimens from the same lot used for the IRFUMA-I irradiation.

More specifically, three spare specimens from the irradiation have been tested and six more have been reconstituted using the broken halves of the first three.

Individual results for the baseline tests are given in Table 7, while the outcome of the Master Curve analyses is provided in Table 8. Experimental points and Master Curves are shown in Figure 17.

Table 7 - Individual results for fracture toughness tests on EUROFER97 in the baseline condition.

Specimen code	T (°C)	W (mm)	B (mm)	a ₀ (mm)	Δa (mm)	K _{Jc} (MPa√m)	DATA VALID
E97-71R	-150	10.005	10.005	5.131	0.00	60.0	YES
E97-71	-140	9.972	9.972	5.221	0.00	60.0	YES
E97-72	-130	9.930	9.999	3.622	0.00	46.8	Precrack invalid
E97-73	-130	9.972	9.972	4.891	0.00	168.7	YES
E97-71L	-100	10.022	10.022	5.276	0.00	89.9	YES
E97-72L	-100	10.190	10.190	5.158	0.00	108.1	NO (K _{Jc} > K _{lim})
E97-72R	-100	10.012	10.012	5.091	0.00	108.0	YES
E97-73L	-100	10.033	10.033	5.098	0.00	103.0	YES
E97-73R	-100	10.017	10.017	5.101	0.00	229.7	NO (K _{Jc} > K _{lim})

Table 8 - Results of the Master Curve analyses for EUROFER97 in the baseline condition.

Option	N	r	K _{o,1TCT} (MPa√m)	K _{med,1TCT} (MPa√m)	T ₀ (°C)
Multi-T	9	6	125.9	116.7	-123

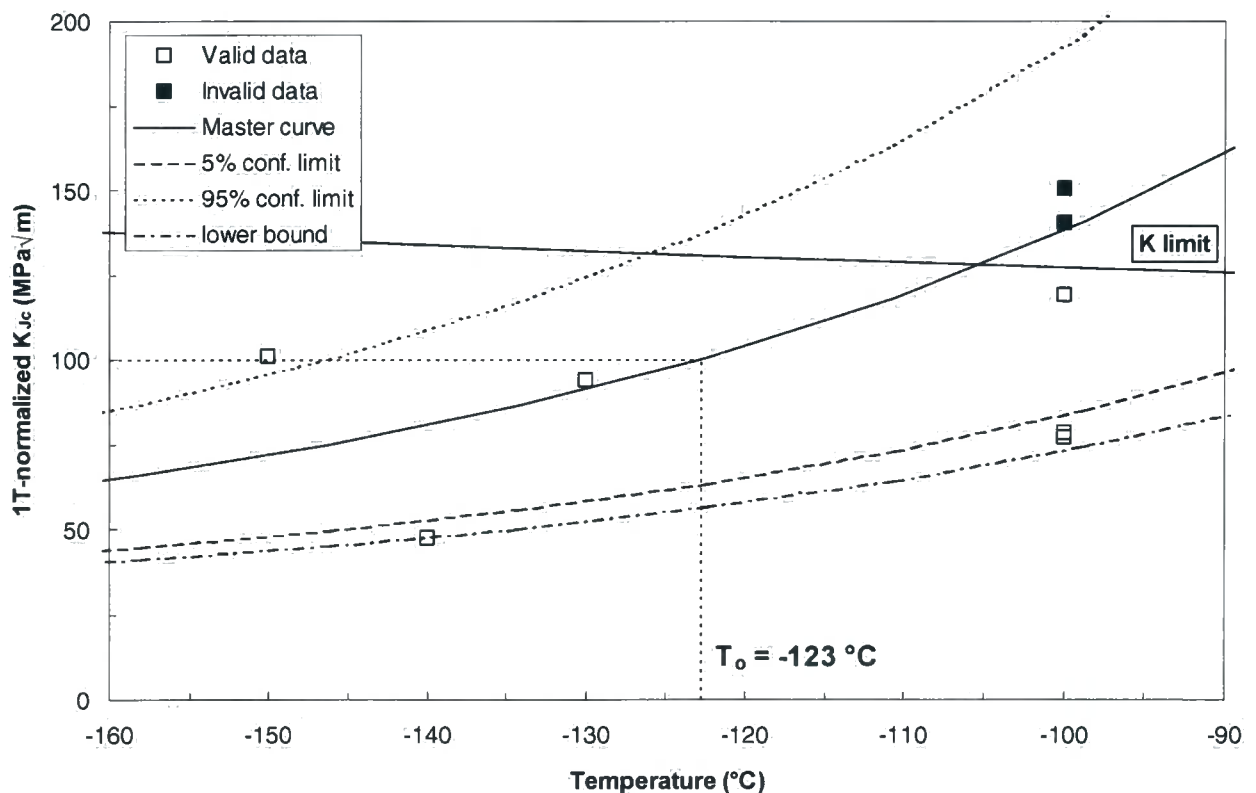


Figure 17 - Fracture toughness results obtained on EUROFER97 in the baseline condition.

One of the unirradiated specimens (code E97-72) exhibited a very irregular and asymmetric fatigue crack growth, as can be seen in Figure 18. The relevant toughness result has not been used in the Master Curve analyses.

Two hypotheses could be suggested to explain this anomalous behaviour:

- a) a strong accidental misalignment of the specimen during the fatigue precracking;
- b) some microstructural feature (inclusion, carbide etc) along the crack front (point B in Figure 18) which could have stopped the crack from propagating in a regular.

However, no evidence was found to corroborate the former hypothesis; in order to investigate the latter, the specimen was subjected to microstructural investigations, which did not however reveal the cause of the irregular fatigue crack growth. Further details have been given in Annex 1.

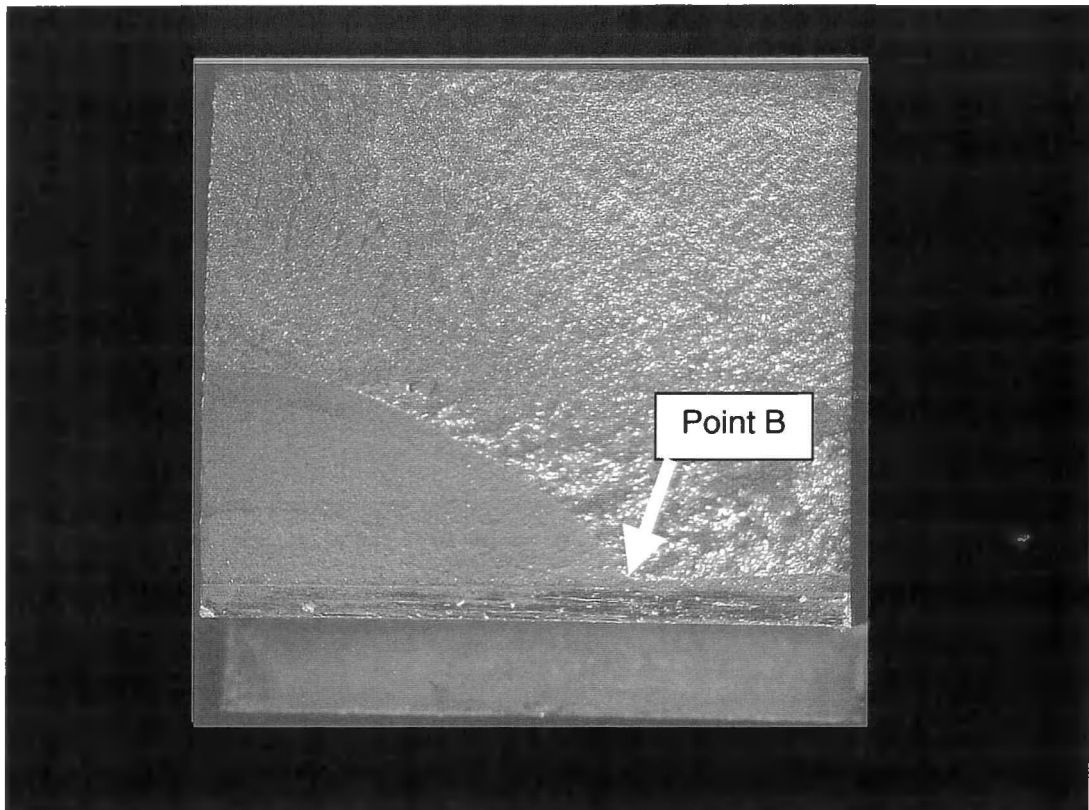


Figure 18 - Fracture surface of unirradiated sample E97-72, showing extremely irregular fatigue crack growth.

The comparison between baseline and irradiated data is presented in Figure 19, where results from NRG and CIEMAT are also reported; SCK•CEN PCCv data have been shifted in temperature to make them comparable to these latter, based on the following assumptions:

- NRG data and Master Curve (from the 25 mm thick plate) have been shifted forward by 22 °C, using the DBTT shift reported for Charpy data [17];
- fracture properties are the same for the bar and the $t = 14$ mm plate (as in the case of tensile and impact properties);
- all SCK•CEN PCCv data have been shifted backwards by 10 °C, on account of the lower constraint with respect to C(T) specimens.

These adjustments are summarised in Table 9.

Table 9 - Adjustments needed for the comparative analysis of fracture toughness data.

Institute	Product form	Condition	Specimen Type	$T_{o,original}$ (°C)	$T_{o,adjusted}$ (°C)	Assumption
CIEMAT	Plate $t = 14$ mm	Unirradiated	C(T)	-132	-132	$T_{o,bar} \equiv T_{o,t=14mm}$
NRG	Plate $t = 25$ mm			-86	-108	$\Delta T_{o,14 \rightarrow 25} \equiv \Delta DBTT$
SCK•CEN	Bar $D = 100$ mm	Irradiated	PCCv	-123	-133	$\Delta T_{o,PCCv \rightarrow CT} = 10$ °C
				-80	-90	

After these adjustments, the Master Curves for baseline data from CIEMAT ($T_0 = -132$ °C) and SCK•CEN ("adjusted" $T_0 = -133$ °C) are practically coincident, whereas the NRG curve ("adjusted" $T_0 = -108$ °C) needs to be further shifted by 25 °C, showing that the difference between the 25 mm thick plate and the other product forms is larger in terms of toughness than in terms of impact properties.

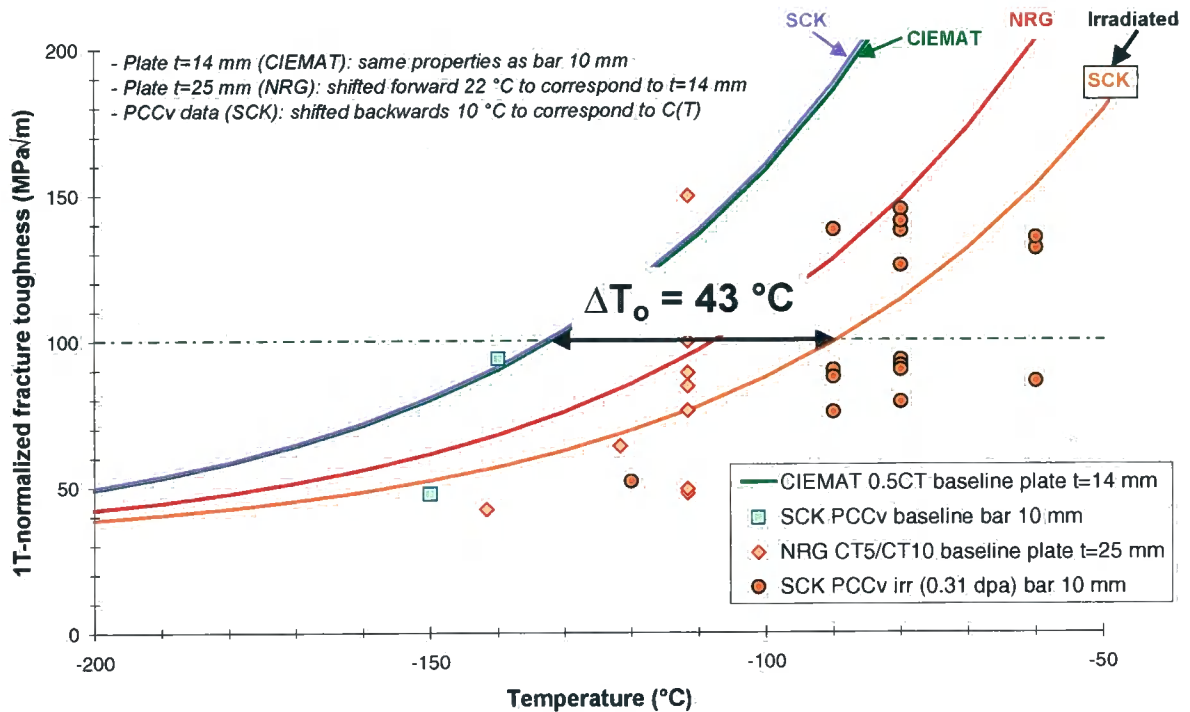


Figure 19 - Comparison between baseline and irradiated fracture toughness data, after the adjustments detailed in Table 9.

Anyway, based solely on the homogeneous data provided by SCK•CEN (bar and PCCv specimens), the irradiation-induced shift of the reference temperature is 43 °C, therefore larger than those measured from the impact tests (14 – 16 °C).

This clearly shows that, if an assessment of the effect of neutron irradiation on the toughness of EUROFER97 or other structural materials has to be made, it is highly advisable to perform actual fracture toughness tests, rather than relying on Charpy impact data, which can provide unconservative evaluations.

6 Summary of irradiation effects and comparison with other RAFM steels

The effects of neutron irradiation under the conditions of the IRFUMA-I experiment (0.32 dpa, $T = 300\text{ }^{\circ}\text{C}$) on the mechanical properties of the RAFM steel denominated EUROFER97 are summarised in Table 10.

Table 10 - Summary of irradiation effects.

Type of test	Dose (dpa)	Parameters measured	Irradiation effect (shift)
Tensile	0.35	Strength Ductility	$\Delta R_{p0.2} \approx 20\%$ - $\Delta R_m = 5 \div 10\%$ (<i>RT to 300 °C</i>) $\Delta \epsilon_u \approx 0\%$ - $\Delta \epsilon_t = 3\% \div 4.5\%$ - $\Delta Z \approx 0\%$
Charpy	0.31	DBTT, USE	$\Delta \text{DBTT} = 14 \div 16\text{ }^{\circ}\text{C}$ - $\Delta \text{USE} = ?$
Toughness	0.31	T_o	$\Delta T_o = 43\text{ }^{\circ}\text{C}$

To assess the significance of such mechanical property changes, comparisons with other RAFM steels from previous "generations" have been performed.

6.1 Tensile properties

As far as mechanical strength is concerned, the consequence of neutron irradiation depends strongly on the irradiation temperature. Below 400 to 500 °C, irradiation-induced microstructural changes lead to lattice hardening, causing an increase in yield stress and ultimate tensile strength and a decrease in uniform and total elongation. The magnitude of the hardening decreases with increasing temperature until it disappears between 400 to 500 °C [31]. Relatively limited data exist for neutron irradiations below 400 °C and doses below 5 dpa [32,33].

As an example, tensile tests on the MANET I steel (a type 11Cr-MoVNb alloy) irradiated in HFR at 250 and 350 °C to about 0.5 to 10 dpa indicated that rapid hardening occurred up to ≈ 1.5 dpa, after which it leveled off; saturation was concluded to occur by ≤ 5 dpa [34,35]. Further tensile tests on the same steel showed that, for irradiation at 300 °C, an increase of 37% for the yield stress and and 31% for the UTS were observed at accumulated doses of about 0.3 dpa [34].

More recently, a collection was published of mechanical test results obtained from several martensitic steels, irradiated at 300 °C up to different doses in the HFR reactor [36]. The steels characterized were F82H mod. (plates, EB-welds and TIG welds), BS-9Cr2WVTa and NF616 (9Cr-0.5Mo-1.8W-V-Nb). Data corresponding to baseline conditions, 2.5 dpa, 5 dpa and in the range 8-12 dpa were reported.

In Figure 20 and Figure 21, NRG baseline [17] and SCK•CEN irradiated tensile data at 300 °C have been superimposed to the original figures in [36], as well as drawing "eyeball" trend curves for the tensile properties of F82H plates. It appears that, with respect to the steels tested and in particular F82H plate materials, EUROFER97 undergoes a significantly larger increase of mechanical strength, whereas ductility is affected to a negligible degree.

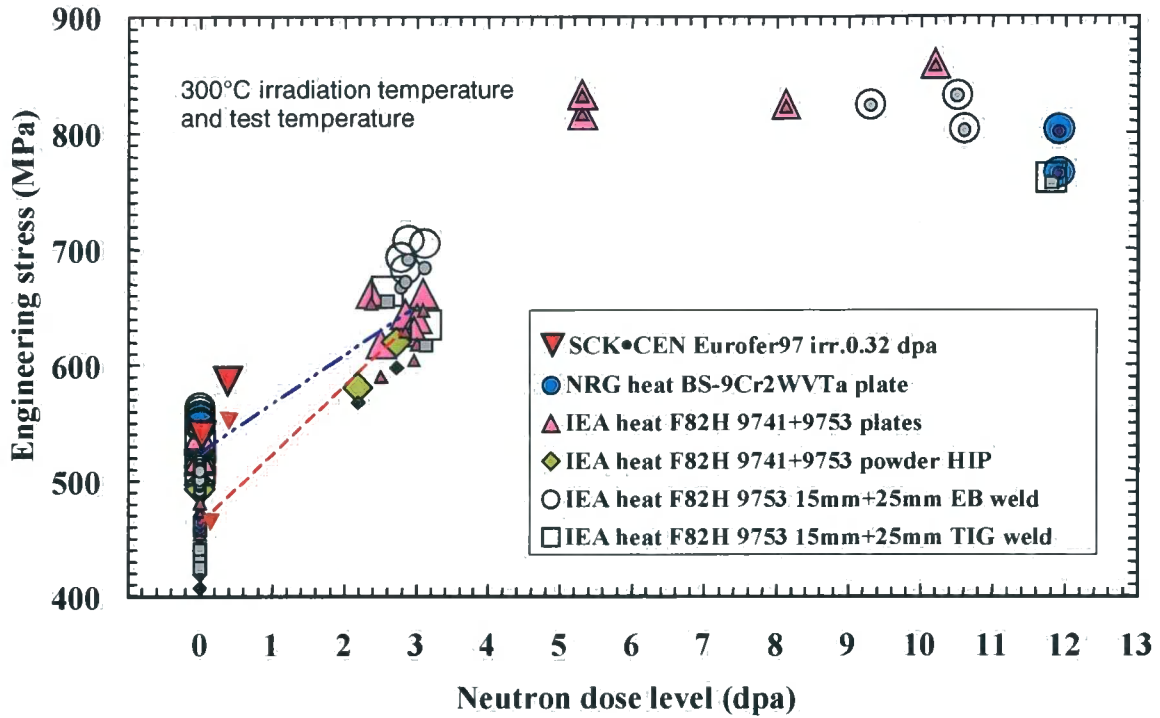


Figure 20 - Engineering stress values for several RAFM steels tested by NRG [36], compared with baseline and irradiated EUROFER97. Small/darker symbols indicate $R_{p0.2}$, large/lighter symbols are for R_m ; red dashed and blue dotted lines are "eyeball" trend lines for F82H plates (yield and UTS, respectively).

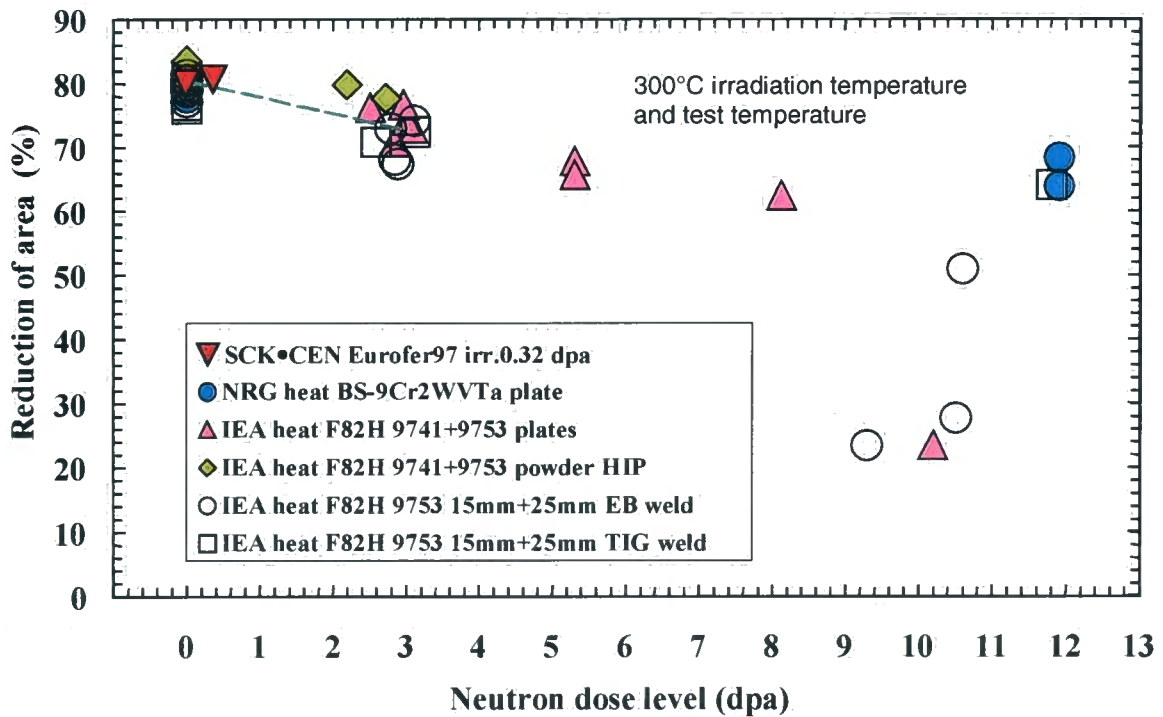


Figure 21 - Reduction of area values for several RAFM steels tested by NRG [36], compared with baseline and irradiated EUROFER97. The green dashed lines is an "eyeball" trend line for F82H plates.

6.2 Impact properties

Irradiation embrittlement of ferritic and ferritic-martensitic steels is related to the hardening caused by the production of dislocation loops, dislocation lines and precipitates during irradiation below 600 °C [37,38]. Hardening is characterized by an increase in flow stress, and, under the assumption that the fracture stress is unaffected by irradiation and that the intersection of the fracture stress curve and the flow-stress curve defines the ductile-to-brittle transition temperature, the increase in flow stress causes a shift in the DBTT [37].

Furthermore, in a fusion reactor, large amounts of transmutation helium will form in the first wall of the structure; the presence of He in the irradiated steel can exacerbate the shift in DBTT [31]. DBTT shift is normally accompanied by a degradation of Upper Shelf Energy.

As in the case of tensile properties, evidence has been found that for most ferritic-martensitic steels the increase in DBTT and the decrease in USE are particularly pronounced below approximately 5 dpa, after which an effect of saturation starts to ensue [39].

For the MANET I steel irradiated in HFR at approximately 290 °C, an increase in DBTT of about 80 °C for 0.3 dpa can be forecast based on accumulated doses of 5, 10 and 15 dpa. On the other hand, irradiation at approximately 490 °C shows substantially no change in transition temperature [40].

The effect of Chromium content on the irradiation-induced DBTT shift has been extensively studied [41]. It was concluded that 8-9Cr steels showed the most promising behaviour, and they were recommended for consideration for "first wall and blanket of fusion reactors". The improved impact behaviour of 9Cr-WV relative to those with greater or lesser Cr contents has been demonstrated in several studies; a minimum of Δ DBTT was observed in the vicinity of 9% Cr [42].

Another extensive study [43] allows to compare the DBTT shift measured on the EUROFER97 irradiated in IRFUMA-I with measurements performed on several other RAFM steels irradiated in HFR under similar conditions (300 °C, 0.2 and 0.8 dpa); the results of such comparisons are given in Table 11 and shown in Figure 22.

Table 11 - DBTT shifts measured on EUROFER97 and other RAFM steels irradiated at 300 °C.

Steel	Dose (dpa)	Δ DBTT (°C)	Reference
EUROFER97	0.31	15	This report
F82H	0.2	15	[43]
	0.8	45	
OPTIFER-Ia	0.2	35	
	0.8	85	
OPTIFER-II	0.2	25	
	0.8	105	
MANET-I	0.2	70	
	0.8	130	
MANET-II	0.2	50	
	0.8	115	
ORNL 3791 (9Cr-2WVTa)	0.2	20	
	0.8	35	

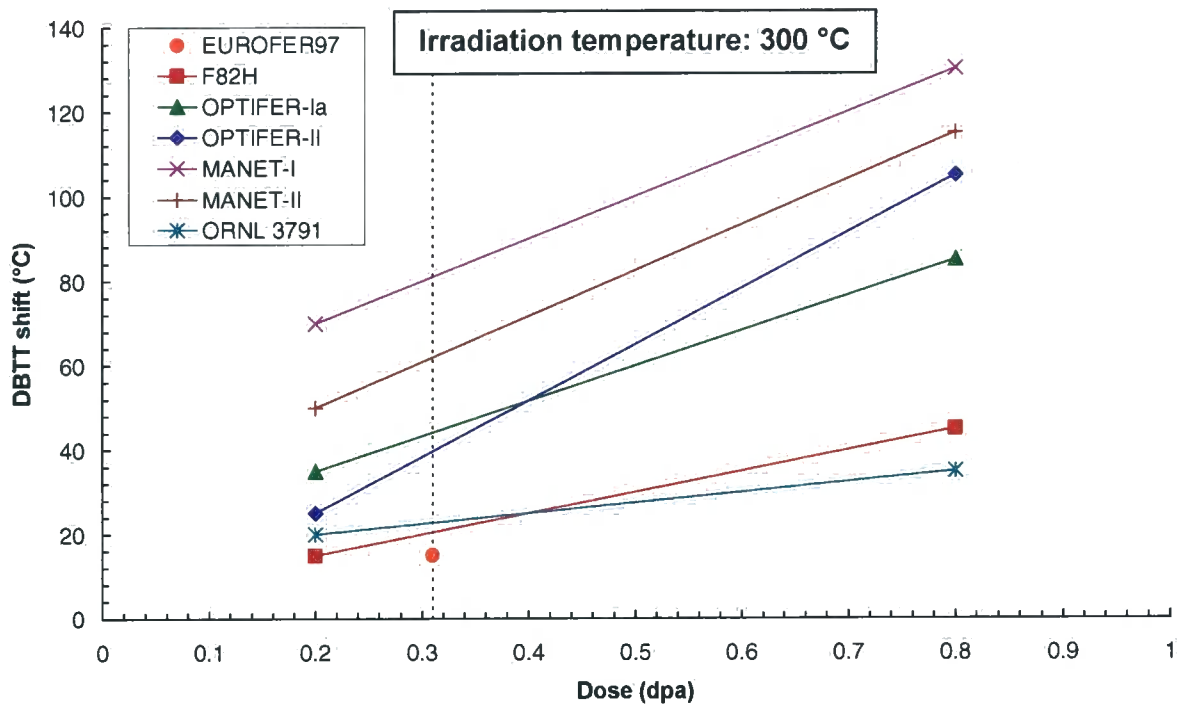


Figure 22 - Comparison between various RAFM steels irradiated at 300 °C, in terms of DBTT shift [43]. Straight lines are just a guide for the eye, and SHOULD NOT be extrapolated to higher doses.

We observe that the performance of EUROFER97 at these low doses is better than all other RAFM steels, although the improvement is moderate with respect to F82H and ORNL 3791.

6.3 Fracture toughness properties

Toughness data for reduced activation steels in the unirradiated and irradiated condition are limited to a few studies on F82H and JLF-1 steels [44-50]. The unirradiated properties are generally similar to those of the conventional Cr-Mo steels [44].

Results from experiments on F82H irradiated to 1.5 to 3 dpa in HFIR [49] and HFR [50] were used to make a comparison of the effect of irradiation on the toughness of HT9 and F82H [49].

In the baseline condition, minor differences were found in the range RT to 300 °C, where failure occurs by ductile tearing and toughness (calculated from J-integral at initiation) for both steels lies between 200 and 300 MPa√m [44].

The 100 MPa√m reference temperature for the unirradiated F82H steel was estimated to be -100 °C [36], about 30 °C higher than for the unirradiated EUROFER97 characterised by CIEMAT [25] and SCK•CEN (this report). Although the data for F82H are limited, irradiation to 1.6 to 2.5 dpa at 250 °C had a much smaller effect than for HT9, in that F82H retained considerable toughness. In the test temperature range investigated, where low uniform elongation was observed in tensile tests, failure in toughness tests occurred by ductile tearing, indicating that tensile embrittlement is not accompanied by embrittlement in the fracture toughness tests [49].

Unfortunately, fracture toughness data on ferritic-martensitic steels irradiated under conditions (temperature and fluence) comparable to those of the IRFUMA-I experiment are presently not available in the open literature.

CONCLUSIONS

Tensile, impact and fracture toughness tests have been performed on the EUROFER97 steel, irradiated in the BR2 reactor at 300 °C up to an accumulated dose of 0.32 dpa.

By comparing test results with data obtained from the unirradiated material, the following has been observed:

- irradiation produces hardening, which can be quantified in the range RT to 300 °C as an increase of 20% for the yield strength and 35% ÷ 55% for the ultimate tensile strength;
- ductility remains satisfactory, with no significant loss in uniform elongation or reduction of area and a slight degradation of total elongation (3% ÷ 4.5%);
- the shift of the DBTT measured from standard Charpy tests is moderate (14 ÷ 16 °C); although no evaluation can be made with respect to the variation of Upper Shelf Energy, the USE value in the irradiated condition remains high, implying that failure in the upper shelf fracture regime should be no concern;
- the shift of the reference temperature (T_0) measured from PCCv toughness tests is higher than for the Charpy DBTT (43 °C), indicating that actual fracture toughness tests have to be performed if a reliable assessment has to be made of the influence of irradiation on the material's toughness.

Comparisons of irradiation effects with respect to other reduced-activation ferritic martensitic steels are limited by the scarcity of data obtained under similar conditions (temperature and/or fluence).

Irradiation hardening was found to be higher than for other RAFM steels (including F82H) in terms of mechanical strength increase, whereas ductility is practically unaffected. As far as irradiation embrittlement (shift of Charpy-based DBTT) is concerned, EUROFER97 appears to perform slightly better than the most recent RAFM steels (specifically, F82H). No relevant data are presently available for fracture toughness.

Further irradiations in the BR2 reactor have already been concluded (IRFUMA II, expected dose ~1.1 dpa, $T = 300$ °C [51]) or are under way (IRFUMA III, expected dose ~2.2 dpa, $T = 300$ °C, [52]), which will allow to assess the effects of higher doses on the mechanical properties of the EUROFER97 steel.

ACKNOWLEDGEMENTS

The Authors would like to acknowledge the professional collaboration of all the technical staff of LHMA, and particularly R. Mertens (cutting scheme and specimen preparation), J. Veraghtert (dimensional controls), J. Schuurmans (tensile tests), R. Vosch (impact tests) and L. Van Houdt (toughness tests).

Sincere thanks also to all the Colleagues who have supplied us their test results on the unirradiated material: J.-W. Rensman (NRG, Petten); A. Alamo (CEA, Saclay), R. Lindau (FZK, Karlsruhe) and P. Fernandez (CIEMAT, Madrid).

REFERENCES

- [1] *Report on the European Materials Assessment Meeting*, Karlsruhe, 5-8 June 2001, edited by EDFA Close Support Unit, Garching (Germany).
- [2] *Proceedings of ITER Materials Assessment Meeting*, 1-5/12/97, ITER, Garching (Germany).
- [3] *Report of the IAEA Workshop / Working Group Meeting on Ferritic/Martensitic Steels for Fusion Applications*, JAERI, Tokyo, Japan, 2-3 November 2000.
- [4] F. Tavassoli, *Present Limits and Improvements of Structural Materials for Fusion Reactors*, to be published in *Journal of Nuclear Materials*, 2002.
- [5] R.L. Klueh, D.S. Gelles, S. Jitsukawa, A. Kimura, G.R. Odette, B. van der Schaaf and M. Victoria, in *10th International Conference on Fusion Reactors*, Baden-Baden, Germany, October 14-19, 2001.
- [6] A.A. Tavassoli, *RAFM Steels – Rules for Design and Inspection*, Annual Report of the Association Euratom/CEA 2000, pp.235-237.
- [7] K. Shiba, *Report of JAERI – Tech – 97 – 038*, JAERI-1998, Tokyo, Japan.
- [8] D.S. Gelles, *Microstructural examination of commercial ferritic alloys at 200 dpa*, *Journal of Nuclear Materials* 233-237 (0) (1996) pp. 293-298.
- [9] A. Uehira, S. Mizuta, S. Ukai and R.J. Puigh, *Irradiation creep of 11Cr-0.5Mo-2W,V,Nb ferritic-martensitic, modified 316, and 15Cr-20Ni austenitic S.S. irradiated in FFTF to 103-206 dpa*, *Journal of Nuclear Materials* 283-287 (0) (2000) pp. 396-399.
- [10] A. Hishinuma, A. Kohyama, R.L. Klueh, D.S. Gelles, W. Dietz and K. Ehrlich, *Current status and future R and D for reduced-activation ferritic/martensitic steels*, *Journal of Nuclear Materials* 258-263 (0) (1998) pp. 193-204.
- [11] S. Revol, S. Launois, R. Baccino, G. Le Marois and B. Rigal, *Development of the elaboration process and joining technologies of R.A.F.M. O.D.S. steels*, *Fusion Engineering and Design* 58-59, 2001, pp. 761 - 765.
- [12] A. Alamo, H. Regle, G. Pons and L.L. Bechade, *Materials Science Forum*, 88-90 (1992) 183.
- [13] E. Lucon, *Mechanical Tests on Two Oxide-Dispersion Strengthened (ODS) Batches of EUROFER97*, SCK•CEN Report BLG-874, March 2001.
- [14] N. Baluc, *Final Report on Task TW1-TTMS-006 Deliverable 7 – Period 01/2001–12/2001*, CRPP Report, Switzerland.
- [15] E. Lucon and M. Wéber, *Irradiation of Mechanical Specimens of EUROFER97 and Chromium Alloys in the BR2 Reactor: the IRFUMA Experiment*, SCK•CEN Report BLG-872, February 2001.

- [16] M. Willekens, *Neutronendosimetrie voor Experiment IRFUMA 1*, SCK•CEN Technische Nota RF&M/Vwi/32.D049011-205/01-14, 2001 (in Dutch).
- [17] H.E. Hofmans, *Tensile and Impact Properties of EUROFER97 Plate and Bar*, NRG Report 20023/00.38153/P, Petten, 15 December 2000.
- [18] R. Lindau and M. Schirra, *First Results on the Characterisation of the Reduced-Activation-Ferritic-Martensitic Steel EUROFER*, 21st Symposium on Fusion Technology (SOFT), Madrid, September 11-15, 2000 (published on Fusion Engineering and Design 58-59, 2001, pp. 781 – 785).
- [19] R. Lindau and M. Schirra, *Status of Investigations on the Thermal and Mechanical Behaviour of EUROFER97*, Workshop on Data Base Evaluation of RAFM Steels, ENEA Brasimone, Italy, November 27-28, 2000.
- [20] A. Alamo, P. Wident, S. Urvoy and Y. Tournier, *Mechanical Properties of EUROFER97 Steel in the As-Received Condition*, CEA Report NT SRMA 01-2419, March 2001.
- [21] M.A. Sokolov and D.J. Alexander, *An Improved Correlation Procedure for Subsize and Full-Size Charpy Impact Specimen Data*, Oak Ridge National Laboratory Report ORNL-6888, NUREG/CR-6379, March 1997.
- [22] E.D. Eason, J.E. Wright and G.R. Odette, *Improved Embrittlement Correlations for Reactor Pressure Vessel Steels*, NUREG/CR-6551, MCS 970501, November 1998.
- [23] C. Fossati et al., *Nota Tecnica CISE NT 80.090*, 1980 (in Italian).
- [24] B. Leis, *Characterizing Dynamic Crack-Resistance of Pipelines Using Laboratory-Scale Practices*, Proceedings of the 3rd International Pipeline Conference 2000, October 1-5, 2000, Calgary, Alberta (Canada).
- [25] P. Fernandez, A.M. Lancha, J. Lapeña, M. Serrano and M. Hernández-Mayoral, *Metallurgical Properties of the Reduced Activation Martensitic Steel EUROFER97 on As-Received Condition and After Thermal Ageing*, 10th International Conference on Fusion Reactor Materials, ICFRM-10, Baden-Baden, Germany, October 14-19, 2001.
- [26] G.R. Odette, H.J. Rathbun, J.W. Rensman and F.P. van den Broek, *On the Transition Toughness of Two RA Martensitic Steels in the Irradiation Hardening Regime: A Mechanism-Based Evaluation*, 10th International Conference on Fusion Reactor Materials, ICFRM-10, Baden-Baden, Germany, October 14-19, 2001.
- [27] K. Wallin, *Quantifying T_{stress} Controlled Constraint by the Master Curve Transition Temperature T_0* , Engineering Fracture Mechanics 68 (3), 2000, pp. 303-328.
- [28] X. Gao, R.H. Dodds, R.L. Tregoning and J.A. Joyce, *Prediction of the T_0 Shift between Specimens of Different Constraints Using the T-Stress Based T-Functions*, International Journal of Fracture 104, L3-L8, 2000.

- [29] E. Lucon and R. Chaouadi, *Radiation Damage Assessment by the Use of Dynamic Toughness Measurements on Pre-Cracked Charpy-V Specimens*, ASTM STP 1405, 2001, pp.68-77.
- [30] E. Lucon, M. Scibetta and E. van Walle, *Application of the Sintap Methodology for Estimating the Fracture Toughness of Reactor Pressure Vessel Steels Based on Charpy Data*, IAEA Specialists' Meeting on Irradiation Embrittlement and Mitigation, Gloucester, UK, 14-17 May 2001.
- [31] R.L. Klueh and D.R. Harries, *High-Chromium Ferritic and Martensitic Steels for Nuclear Applications*, ASTM Mono 3, 2001.
- [32] V.S. Agueev et al., in *Effects of Radiation on Materials: 14th International Symposium*, ASTM STP 1046, Vol.I, 1989, 98.
- [33] P.J. Maziasz, R.L. Klueh and J.M. Vitek, *J. Nucl. Mater.* 141-143 (1986) 929.
- [34] K. Ehrlich, D.R. Harries and A. Möslang, *Characterisation and Assessment of Ferritic/Martensitic Steels*, Forschungszentrum Karlsruhe, FZKA Report 5626, February 1997.
- [35] M.I. deVries, in *Effects of Radiation on Materials: 16th International Symposium*, ASTM STP 1175, 1993, 558.
- [36] J. Rensman et al., *Tensile Properties and Transition Behaviour of RAFM Steel Plate and Welds Irradiated Up to 10 dpa at 300 °C*, 10th International Conference on Fusion Reactor Materials, ICFRM-10, Baden-Baden, Germany, October 14-19, 2001.
- [37] J.R. Hawthorn, in *Treatise on Materials Science and Technology*, Vol. 25, Academic Press, New York, 1983, 461.
- [38] G.E. Lucas and D.S. Gelles, *Journal of Nuclear Materials* 155-157, 1988, 164.
- [39] R.L. Klueh and D.J. Alexander, *Journal of Nuclear Materials* 258-263, 1998, 1269.
- [40] M. Rieth et al., *Fusion Engineering and Design* 29, 1995, 365.
- [41] V.V. Rybin, I.P. Kursevich and A.N. Lapin, *Journal of Nuclear Materials* 258-263, 1991, 1324.
- [42] A. Kohyama et al., *Journal of Nuclear Materials* 233-237, 1996, 138.
- [43] M. Rieth, B. Dafferner and H.D. Röhrig, *Journal of Nuclear Materials* 258-263, 1998, 351.
- [44] G.E. Lucas et al., in *Effects of Radiation on Materials: 17th International Symposium*, ASTM STP 1270, 1996, 790.
- [45] H.-X. Li et al., *Journal of Nuclear Materials* 233-237, 1996, 258.

- [46] H.-X. Li et al., *Fusion Materials Semiannual Progress Report for Period Ending December 31, 1996*, U.S. Department of Energy, DOE/ER-0313/21, April 1997, p.142.
- [47] A. Nishimura, N. Inoue and T. Muroga, *Journal of Nuclear Materials*, 258-263, 1998, 1242.
- [48] K. Shiba, *Proceedings of the IEA Workshop/Working Group Meeting on Ferritic/Martensitic Steels*, Petten, The Netherlands, October 1-2, 1998, ORNL/M-6627.
- [49] A.F. Rowcliffe et al., *Journal of Nuclear Materials*, 258-263, 1998, 1275.
- [50] M. Horsten, *Proceedings of the IEA Working Group Meeting on Ferritic/Martensitic Steels*, Culham, UK, October 24-25, 1996, ORNL/M-5674.
- [51] E. Lucon and M. Wéber, *Irradiation of Mechanical Specimens of EUROFER97 in the BR2 Reactor: the IRFUMA-II Experiment*, SCK•CEN Report BLG-910, February 2002.
- [52] M. Wéber, *IRFUMA III: Summary Report*, SCK•CEN Internal Memo MI.57/F040103/85/MW.rw, 4/2/2002.

APPENDIX 1

**INSPECTION CERTIFICATE
ISSUED BY BÖHLER FOR EUROFER97
(HEAT N° E83699)**

QS


BÖHLER
 EDELSTAHL

Page 1 of 4

INSPECTION - CERTIFICATE NO.	: 029060
ABNAHMEPRÜFZEUGNIS NR.	:
acc. to/nach EN 10204/3.1B	

Customer	: THE COMMISSION OF THE
Besteller	: EUROPEAN COMMUNITY
Order-No.	: Contract ERB 5004 CT 980018
Kunden Best. Nr.	:
Böhler-Order-No.	: 998.790 dd. 98-11-03
Böhler Auftrags Nr.	:
Material	: "Böhler Z-T512" = EUROFER 97
Werkstoff	: forged, heat-treated, peeled, polished, IT k12
	: geschmiedet, vergütet, geschält, poliert IT k12
Requirements	: NET 97-917, TMP/DHP-No. 98338 Rev. 0;
Anforderungen	:

Description of Stores:
Materialverzeichnis:

Bars Stück	Dimension Abmessung mms/mm	Heat-No. Schmelze Nr.	Test-No. Probe Nr.
6	Ø 100	E83699	E483

Chemical Composition: (Heat-Analysis %)
Chemische Zusammensetzung: (Schmelzenanalyse %)

Heat-No Schmelzen Nr.	Test-No Probe Nr.	C	Si	Mn	P	S	Cr	Mo	Ni
E83699	B/B	0,12	0,07	0,43	<0,005	0,004	8,93	<0,001	0,007
	TE/SR	0,12	0,07	0,44	<0,005	0,004	8,99	<0,001	0,007
	TC/SM	0,12	0,07	0,44	<0,005	0,004	8,99	<0,001	0,007

Heat-No Schmelzen Nr.	Test-No Probe Nr.	V	W	Cu	Co	Ti	Al	Nb
E83699	B/B	0,19	1,10	0,022	0,004	0,008	0,008	<0,001
	TE/SR	0,19	1,10	0,021	0,004	0,009	0,008	<0,001
	TC/SM	0,19	1,10	0,022	0,004	0,009	0,008	<0,001

INSPECTION-CERTIFICATE-NO. : 029060
 ABNAHMEPRÜFZEUGNIS-NR. :



Page/Seite 2 of 4

Heat-No Schmelzen Nr.	Test-No Probe Nr.	B	N	Pb	Ta	O	As	Sn
E83699	B/B	<0,001	0,019	<0,0003	0,13	0,0012	<0,005	<0,005
	TE/SR	<0,001	0,016	<0,0003	0,14	0,0010	<0,005	<0,005
	TC/SM	<0,001	0,017	<0,0003	0,14	0,0013	<0,005	<0,005

Heat-No Schmelzen Nr.	Test-No Probe Nr.	Zr	Sb
E83699	B/B	<0,005	<0,005
	TE/SR	<0,005	<0,005
	TC/SM	<0,005	<0,005

B = Bottom

TE = Top edge

TC = Top center

B = Boden

SR = Schopf Rand

SM = Schopf Mitte

Deviations accepted by the client/Abweichungen vom Kunden toleriert

Cleanliness test acc. to ASTM E45/A :
Schlackenauswertung nach ASTM E45/A :

from the ingot / vom Block

Test No.	A		B		C		D	
	thin	heavy	thin	heavy	thin	heavy	thin	heavy
B/B	-	-	0,5	-	-	-	1,0	-
TE/SR	-	-	-	-	-	-	1,0	-
TC/SM	-	-	-	-	-	-	1,0	0,5

from the bars / von den Stäben

Spec./Vorschr. A,B,C,D ≤ 1

Test No.	A		B		C		D	
	thin	heavy	thin	heavy	thin	heavy	thin	heavy
S1	-	-	0,5	-	-	-	1,0	0,5
S1/3	-	-	0,5	-	-	-	1,0	0,5
S3/3	-	-	0,5	-	-	-	1,0	0,5
B3/3	-	-	0,5	-	-	-	1,0	0,5
B2/3	-	-	1,0	-	-	-	1,0	0,5
B2	-	-	-	-	-	-	1,0	0,5

Remark: see enclosed Supplement 1

Bemerkung : siehe Beilage 1

Heat-treatment / Wärmebehandlung:

Hardening/Härten:	979°C – 1 h 51 min. – Air/Luft
Tempering/Anlasse:	739°C – 3 h 42 min. – Air/Luft

Remark: see enclosed Supplement 2

Bemerkung : siehe Beilage 2

INSPECTION-CERTIFICATE-NO. : 029060
 ABNAHMEPRÜFZEUGNIS-NR. :

Page/Seite 3 of 4



Chemical Composition: (Check Analysis %)
Chemische Zusammensetzung: (Stückanalyse %)

Test No.	C	Si	Mn	P	S	Cr	Mo	Ni	V	W	Cu	Co
Specif. Vorschr.	0,09 0,12	max. 0,05	0,20 0,60	max. 0,005	max. 0,005	8,50 9,50	max. 0,005	max. 0,005	0,15 0,25	1,0 1,2	max. 0,005	max. 0,005
S1	0,12	0,06	0,42	0,004	0,003	8,87	<0,001	0,0075	0,19	1,10	0,021	0,005
	Ti	Al	Nb	B	N	Ta	O	As	Sn	Sb	Zr	
Specif. Vorschr.	max. 0,01	max. 0,01	max. 0,001	max. 0,001	0,015 0,045	0,05 0,09	max. 0,01	As+Sn+Sb+Zr = max. 0,05				
S1	0,008	0,008	<0,001	<0,0005	0,018	0,14	0,0013	<0,005	<0,005	<0,005	<0,005	

Deviations accepted by the client/Abweichungen vom Kunden toleriert

Mechanical Properties/Mechanische Eigenschaften :

Tensile-Test / Zugversuch :

Test-No. Probe-Nr.	Temp. °C	0,2% Proof Str 0,2% Dehngr. N/mm ²	Tensile Str. Zugfestigt. N/mm ²	Elongation Dehnung (l = 5d)%	Reduction Einschnürung %
Spec./Vorschr.	RT	min.500	min.600	min.15	inf.
E483/1	RT	548	690	21	74
Spec./Vorschr.	550	min.300	inf.	inf.	inf.
E483/2	550	367	418	18	86

Impact-Test / Kerbschlagbiegeversuch :

Test-No. Probe-Nr.	Temp. °C	Impact-Energy Kerbschlagarbeit Charpy-V/J
Spec./Vorschr.	+20	inf.
E483/3	+20	203, 212, 205
Spec./Vorschr.	0°	inf.
E483/4	0°	174, 196, 200
Spec./Vorschr.	-20	inf.
E483/5	-20	158, 155, 167

Grain size acc. ASTM E 112 :
Korngröße gem. ASTM E 112 :
 Spec./Vorschr. ≥6

Edge - Center : 10
 Rand - Mitte : 10

INSPECTION-CERTIFICATE-NO. : 029060
 ABNAHMEPRÜFZEUGNIS-NR. :

Page/Seite 4 of 4



Ferrite-Content acc. AMS 2315 :
Ferritgehalt gem. AMS 2315 :
 Spec./Vorschr.: max. 3%

Edge - Center : 0%
 Rand - Mitte : 0%

Hardness-Vickers :
Vickershärte :
 Spec./Vorschr. : 200 - 240 HV

Edge	D/4	Center	D/4	Edge
Rand	D/4	Mitte	D/4	Rand
227	221	220	217	220 HV

Dimensional control on all bars :
Maßkontrolle an allen Stäben :


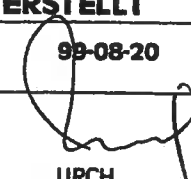
Ø 100 ^{+0.2} mms

Ultrasonic examination on all bars acc. SEP 1923 : satisfactory
Ultraschallprüfung an allen Stäben gem. SEP 1923 : Gutbefund

Visual Testing : satisfactory
Visuelle Kontrolle : anzeigenfrei

Remark : see enclosed Supplement 1 + 2
 Bemerkung : siehe Beilage 1 + 2

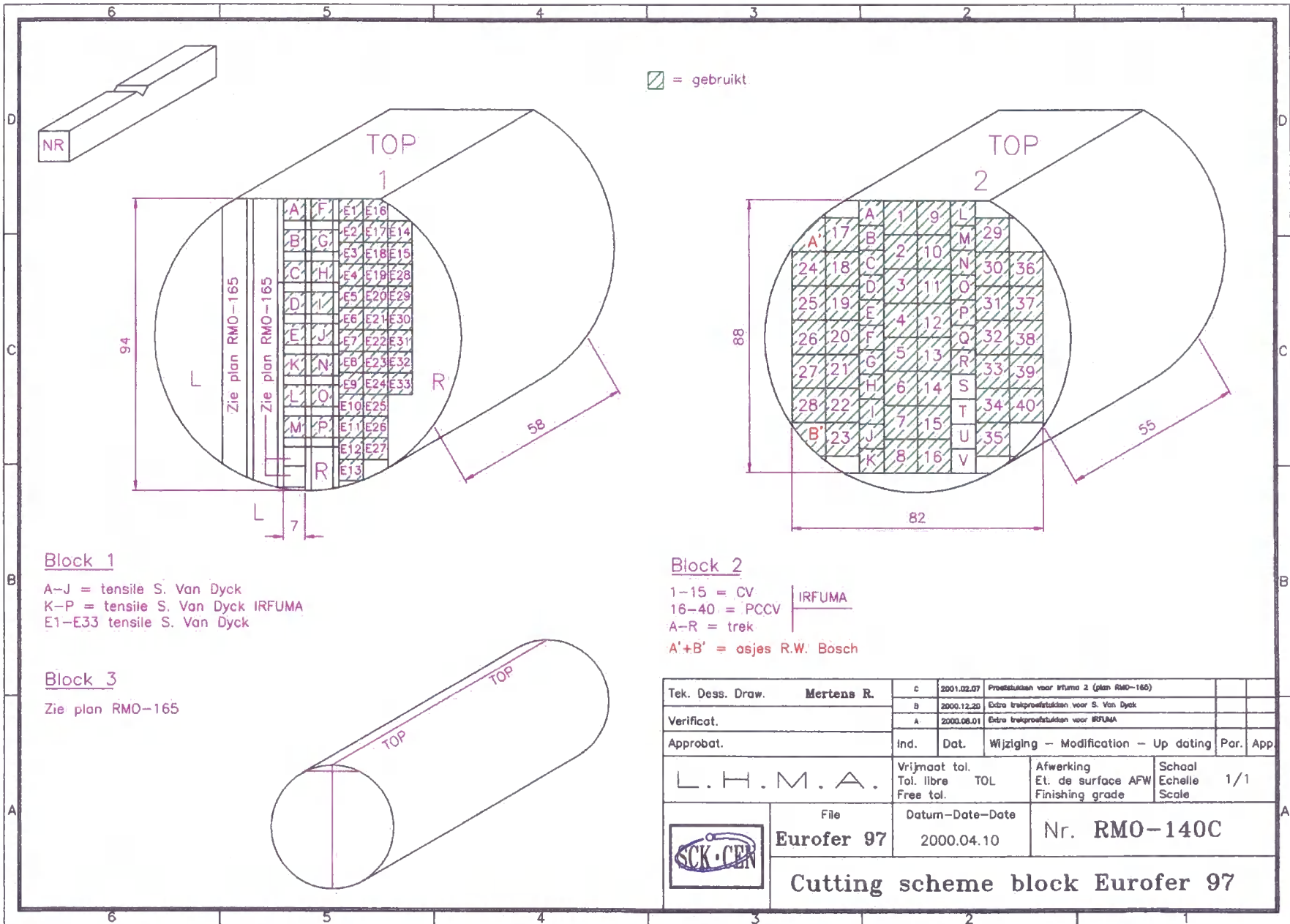
BÖHLER EDELSTAHL GMBH
 KAPFENBERG WORKS / WERK

APPROVED GEPRÜFT	PREPARED ERSTELLT
DATE DATUM 99-08-20	DATE DATUM 99-08-20
SIGNATURE UNTERSCHRIFT  LEITGER	SIGNATURE UNTERSCHRIFT  URCH
QUALITY/ASSURANCE QUALITÄTSSICHERUNG	ACCEPTANCE INSPECTION/CERTIFICATION ABNAHME

171.140 present print P. 04/01/00/00/00/00

APPENDIX 2

CUTTING SCHEME FOR EUROFER97 (FORGED BAR, HEAT N° E83699)



ANNEX 1

**Microstructural Investigations on
the unirradiated sample E97-72**

by A. Leenaers

A1. Introduction

Sample E97-72 (precracked Charpy-V specimen) showed an irregular pattern in the fatigue precracked surface. It was hoped that microscopic analysis could reveal the cause of this anomalous behaviour.

On the fracture surface, Scanning Electron Microscopy (SEM) combined with Energy Dispersive Analysis (EDX) has been performed. Next, the fractured surface has been polished and a grain etch was performed. The etched surface was examined using SEM and optical microscopy.

A2. Results

A2.1 SEM : Secondary Electron Image

Figure A 1 gives an overview of the fracture surface. Several areas with different morphology can be distinguished:

- precracked zone : zone A and a more porous zone D
- fracture ligament zone : zones C and B.

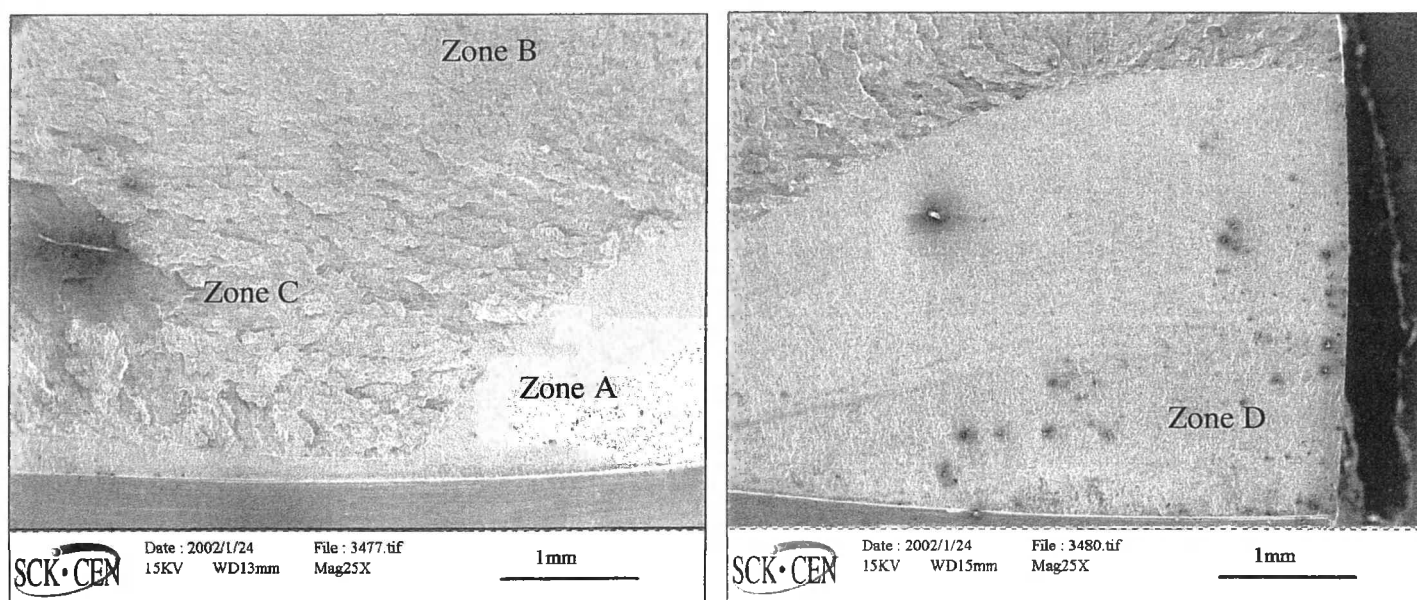
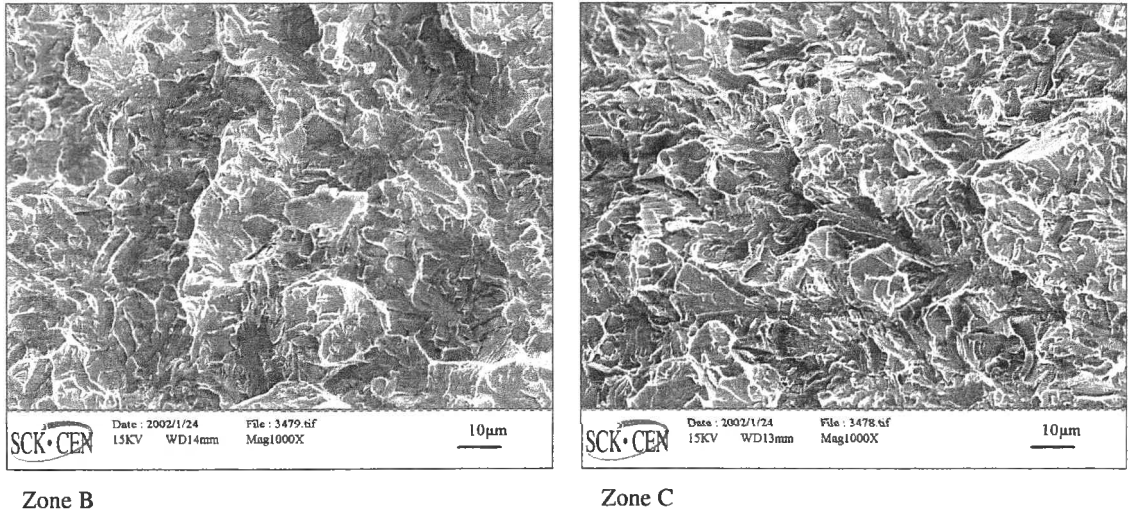


Figure A 1 - The specimen surface can be divided into larger zones : precrack zones A and D, ligament zones B and C.

A more detailed image of the ligament (Figure A 2) reveals that zones B and C differ merely in the direction of fracture rather than in composition or morphology.



Zone B

Zone C

Figure A 2 – Detailed images of the morphology of the ligament (zones B and C).

During further analyses, a fifth zone could be identified at the base of the precrack (zone E, Figure A 3).

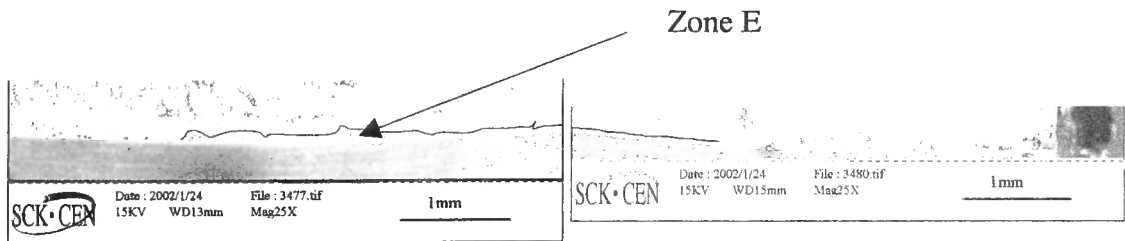


Figure A 3 – A fifth region can be defined at the base of the precrack (Zone E).

From the secondary electron images, no differences in morphology (such as grain structure, precipitates, etc) in any of the zones could be found.

3. Energy dispersive analysis : chemical analysis

The x-ray spectra of the individual zones (defined by the secondary electron images) have been measured using energy dispersive analysis (Figure A 4). These spectra can be used to quantify the chemical composition (Table A 1).

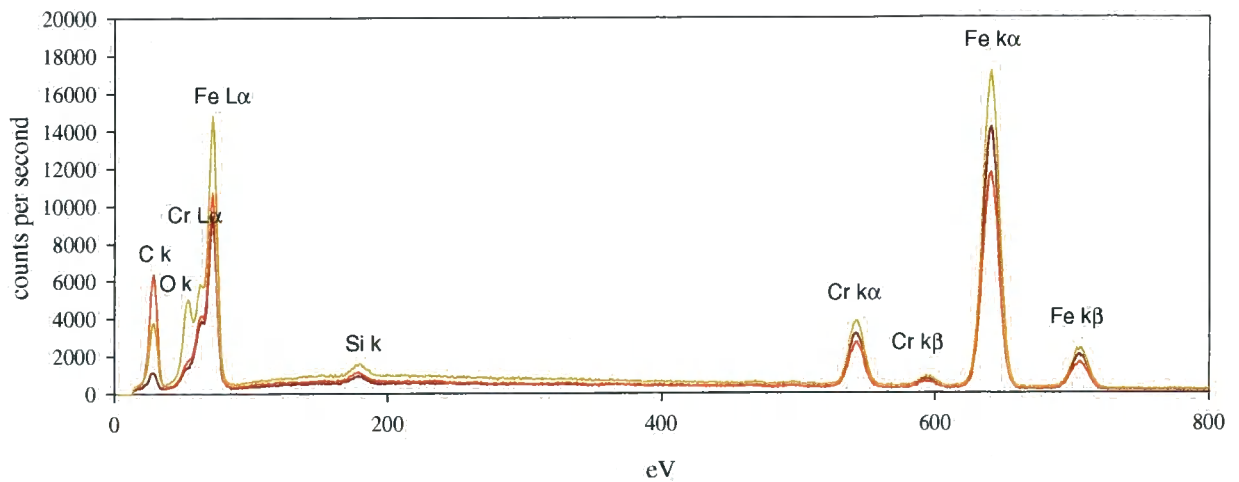


Figure A 4 - X-ray spectra revealing the chemical composition of several zones of the Eurofer97 specimen.

Table A 1 - Chemical analysis in the different zones. Due to systematic errors, these values are associated to an uncertainty of about 5-10% weight percent. (< = under the resolution limit of the machine.)

Wt%	Fe	Cr	Mn	V	W	Ta
Zone A	88.0	9.8	-	-	-	-
Zone B	88.1	9.7	0.56	0.34	1.37	<
Zone C	88.1	9.7	0.73	0.20	1.13	0.15
Zone D	87.8	9.8	0.26	0.13	1.42	<
Zone E	85.7	9.5	0.60	0.19	1.50	<

As can be seen from Table A 1, the chemical composition of the different zones is almost identical. Only in zone E (at the base of the precrack), a slight increase in oxygen concentration is observed.

4. Energy dispersive analysis : x-ray mapping

Often it is desirable to analyse variations in the x-ray intensity of one or more selected elements across a two dimensional area (map).

The x-ray mapping (Figure A 5) contains part of the zone E. Also here a slight increase in oxygen concentration is observed.

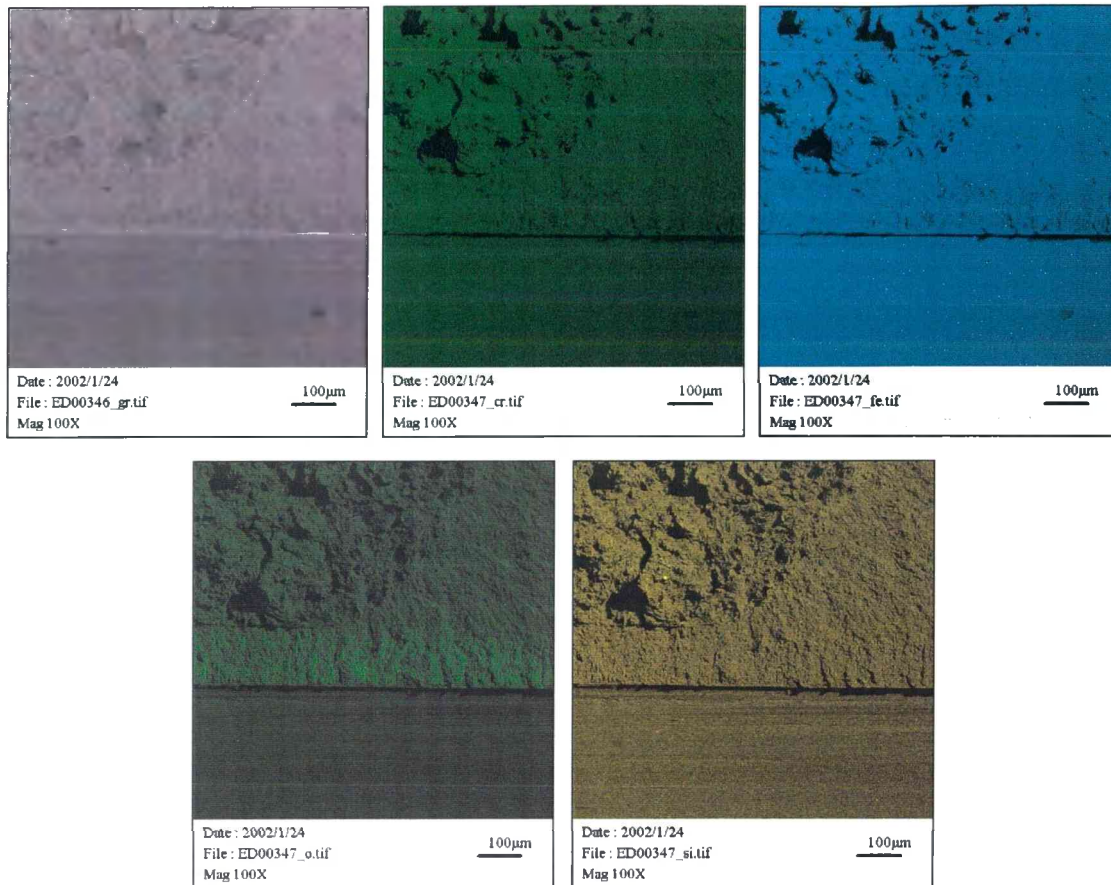


Figure A 5 – From top to bottom, left to right : SE image of the area, Cr K α X-ray map, Fe K α x-ray map, O K α x-ray map and Si K α x-ray map.

5. Grain etching

The mechanical properties of EUROFER97, which has a tempered martensitic structure, can be affected by material defects like additional phases (δ -ferrite stringers) or high concentrations of inclusions. These latter can be traced using the SEM/EDX technique. Additional phases like δ -ferrite stringers are more easy to identify by applying a grain etch to the polished surface.

The etchant used is Vilella's reagent, which contains 1 g picric acid, 5 ml HCL, 100 ml ethanol. The etching is done at room temperature by immersing the polished surface for 15 sec. Vilella's reagent etches martensite and outlines secondary phase particles like carbides and/or δ -ferrite.

Optical microscopy images and secondary electron images of the etched specimen fracture surface are shown in Figure A 6 and Figure A 7.

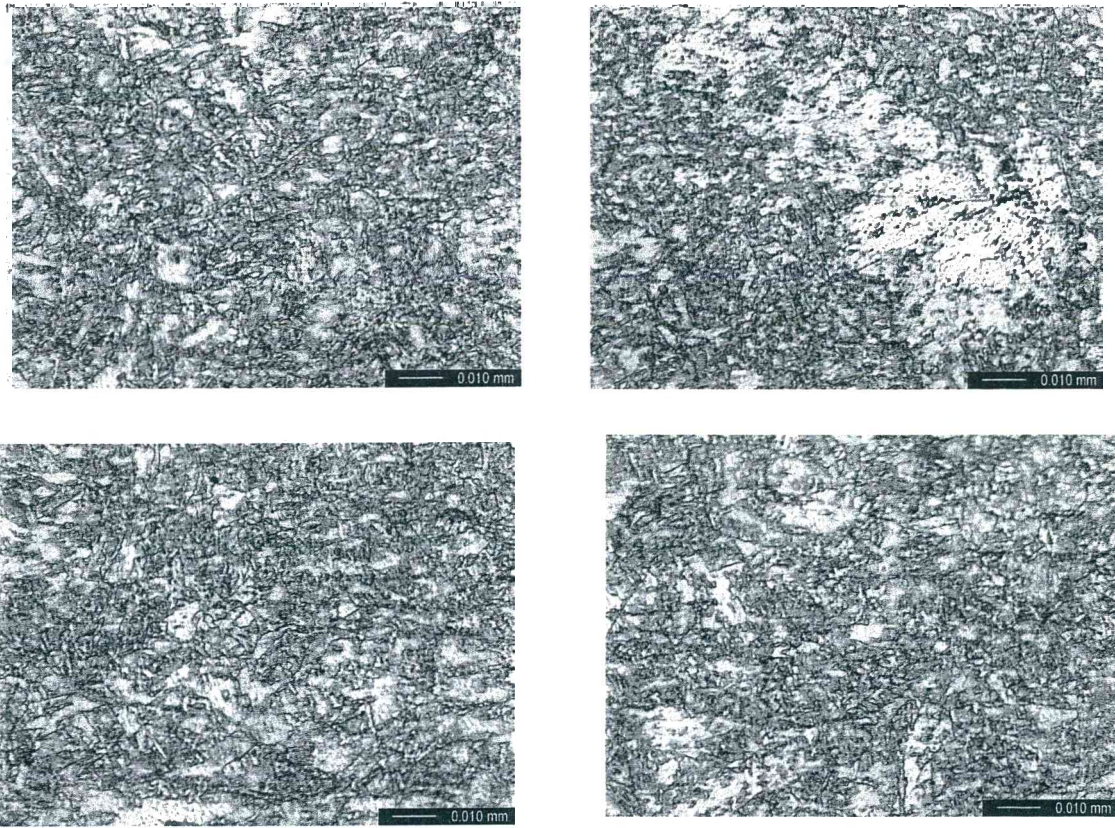
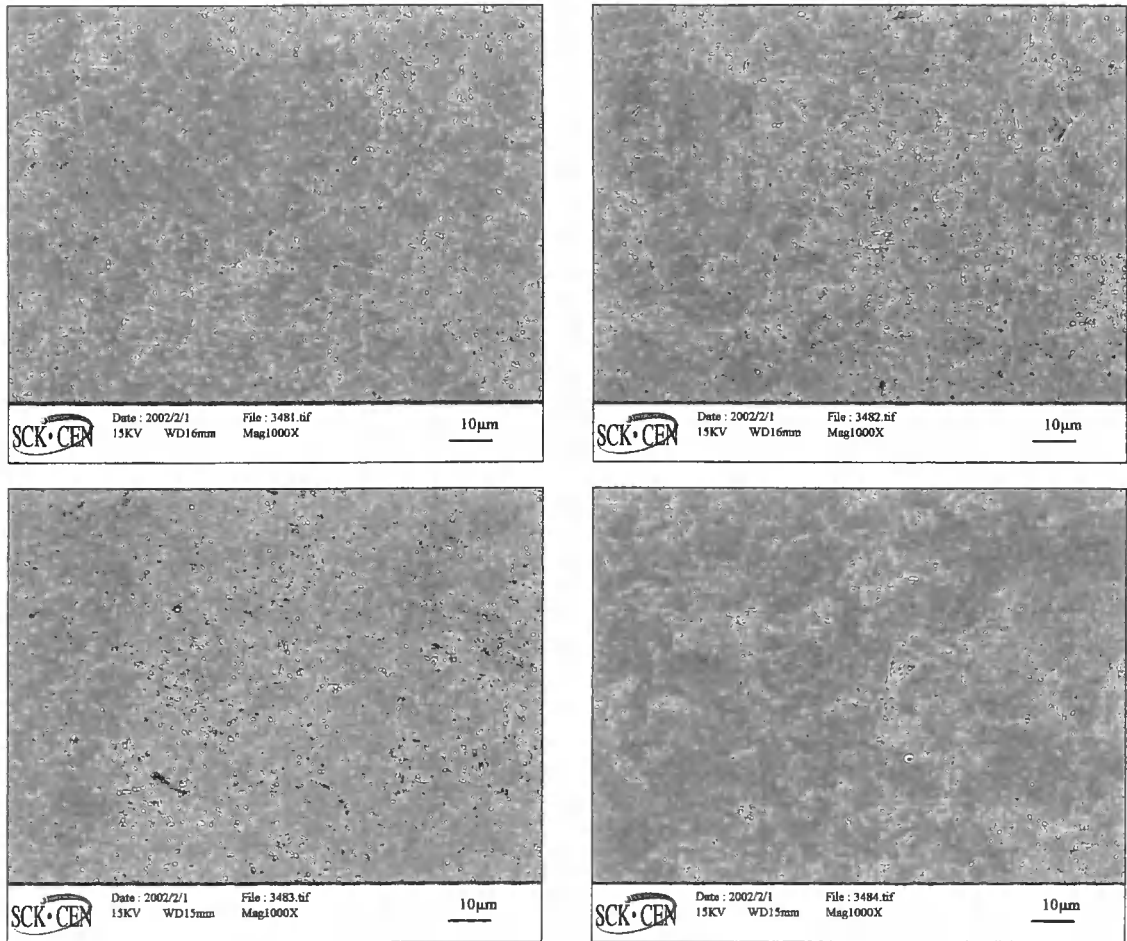


Figure A 6 - *Optical microscopy images at the corners of the specimen surface in etched condition.*

All positions on the surface show a rather fine homogeneous martensitic matrix with small prior austenite grains (approximate size: 10 μm). No indication of secondary phases or particles can be observed.



Position of images on specimen

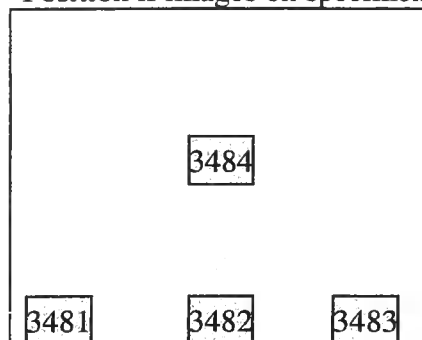


Figure A 7 - Secondary electron images of the specimen surface in etched condition.

Conclusion

From the microstructural analyses performed, no clear explanation has been found for the anomalous behaviour shown by the specimen during fatigue precracking.

